6-30-1966

Effects of non-constant molal flow on distillation plate separation

Joseph Lawrence Niedzwiecki
New Jersey Institute of Technology

Recommended Citation

Niedzwiecki, Joseph Lawrence, "Effects of non-constant molal flow on distillation plate separation" (1966). *Theses*. 2766.
https://digitalcommons.njit.edu/theses/2766

EFFECTS OF NON-CONSTANT MOLAL FLOW ON DISTILLATION PLATE SEPARATION

BY

J. L. NIEDZWIECKI - W. WEISSMAN

A THESIS
PRESENTED IN PARTIAL FULFILLMENT OF
THE REQUIREMENT FOR THE DEGREE
OF
MASTER OF SCIENCE IN CHEMICAL ENGINEERING
AT
NEWARK COLLEGE OF ENGINEERING

NEWARK, NEW JERSEY

JUNE, 1966

ABSTRACT

This thesis presents new equations for predicting degree of separation on a distillation plate, recognizing non-constant molal flow effects. A FORTRAN program is included for solving the new equations. Experimental runs were made for comparison to theoretical predictions.

First an equation is derived for predicting separation at a point on a distillation plate. The derivation is analogous to Murphree's point efficiency equation except that the effects of flow between phases are included by applying the Colburn-Drew theory. Finally, an overall plate separation equation is derived analogous to the A.I.Ch.E. eddy diffusion model for Murphree plate efficiency, except that the rate of flow between phases is included in the differential material balance .

Data were taken at varying degrees of condensation on a distillation plate for the system water-toluene. Conclusive proof on the validity of the equations could not be drawn from the data due to sample contamination and analytical inaccuracy. The data do, however, exhibit a definite trend in the direction predicted by the new equations.

The new equations are recommended for use on the basis of their being derived on a more fundamental basis than the Murphree point and plate efficiency equations. The same basic data are used as in predicting Murphree efficiencies and thus the new technique offers the advantage of giving a more fundamental prediction without needing any additional information about the particular system involved.

APPROVAL OF THESIS

FOR

DEPARTMENT OF CHEMICAL ENGINEERING

NEWARK COLLEGE OF ENGINEERING

BY

FACULTY COMMITTEE

APPROVED:

NEWARK, NEW JERSEY

JUNE, 1966

ACKNOWLEDGMENT

The authors wish to express their appreciation to Dr. J. E. McCormick for his helpful assistance and thoughtful review of this work.

TABLE OF CONTENTS

LIST OF TABLES AND FIGURES

I. INTRODUCTION

Distillation separation is one of the most important unit operations employed in todays chemical and petroleum plants. The distillation plate is the building block of a distillation column and fundamental separation predictions are made by plate-to-plate calculations. These calculations can be done by assuming the tower consists of ideal, or theoretical, plates or by dealing directly with the actual plates.

The majority of tower designs are presently made by dealing with theoretical plates. Deviations from equilibrium are accounted for by use of an (ideal plates/actual plates) efficiency (E_o). The value of E_o is normally determined by first predicting the degree of separation achieved between key components on actual plates in the distillation column. This degree of separation, expressed as the Murphree vapor efficiency of approach to equilibrium [$E_{MV} = (y_2-y_1)/(mx_2-y_1)$], is predicted from mass transfer and tray mixing relationships. E_o is then predicted from E_{MV} by an expression derived for a tower section in which stream rates and component equilibrium constants are fixed.

In certain types of distillation predictions the concept of equilibrium stages does not offer a satisfactory basis for calculation. In multicomponent systems, for example, a problem that often occurs is that of predicting leaving stream compositions for non-key, low efficiency components. For these components the number of theoretical plates required are far less than for the key components and accurate predictions require actual plate-to-plate calculations. At present, Murphree vapor efficiencies (E_{MV}) are used in these calculations. This is not entirely satisfactory because this efficiency is based on the assumption that no net condensation or vaporization occurs on the distillation plates. In sections of some towers large deviations from constant molal overflow occur, i.e., in petroleum refinery self-refluxed gasoline deethanizers, up to 70 percent of the vapor entering the top tray is condensed on that tray.

Scope of Thesis

The intent of this thesis is to: (1) develop theoretical expressions for the degree of separation between leaving streams on a distillation plate, recognizing the effects of non-constant molal flow, and (2) compare predictions from these expressions with experimental data. The distillation system selected was the removal of water from toluene. A water stripping experiment was chosen because water is one of the chief non-key, low efficiency components in refinery distillations which must be traced by actual plate-to-plate calculations.

Work by Previous Investigators

Murphree(1) is credited with developing the first mathematical models for determining the approach to equilibrium on an actual distillation plate. Murphree did his work in the belief that "the concept of the theoretical plate does not offer a satisfactory basis of calculation for rectifying columns where the mixture being rectified contains more than two components, and even for some calculations on binary mixtures its use is not satisfactory." He based his equations on the assumption of constant molal flow in order to simplify the plate-to-plate calculations which at that time had to be done by hand. To compensate for the assumption of constant molal flow in actual systems, Murphree recommended taking the molal latent heat of vaporization for one of the components as a basis and assigning artificial molecular weights to other components. In this manner, the molal latent heats corresponding to these artificial "moles" are equal to the molal latent heat of the base component.

Murphree assumed mass transfer occurs by diffusion as a vapor bubble rises through the liquid on a plate. He devised two different models to relate the equilibrium approach to the diffusional mass transfer properties. The Murphree vapor efficiency model assumes the vapor entering the plate is homogeneous in composition and there are no concentration gradients in the liquid on the plate. The Murphree liquid efficiency model is also based on homogeneous vapor to the plate but the liquid is assumed to undergo a progressive linear change in composition across the plate. Today, most distillation plate separation prediction procedures assume that the Murphree vapor efficiency is applicable to vertical slabs of differential length along the plate. The efficiency of a differential slab is called the Murphree vapor point efficiency (E_{OG}). The effect of liquid mixing on the plate is brought into account by predicting a Murphree vapor plate efficiency (E_{MV}) as a function of E_{OG} and mixing parameters.

The heat transfer associated with condensation and vaporization on a distillation plate affects the gas/liquid interface temperature and hence the equilibrium constant at the interface. Nord(2) experimented with determining vapor and liquid temperature efficiencies analogous to Murphree vapor and liquid composition efficiencies, and compared values with Murphree efficiencies. No attempt was made, however, to bring in the effects of non-constant molal flow on diffusional transfer. Determination of experimental temperature efficiencies was difficult because of heat transfer through surfaces other than the gas/liquid interface.

No further consideration of the effects of non-constant molal flow on distillation plate separation appears in the literature; however, such effects have been considered for other fractionation equipment. Treybal(3) considered a packed absorption column in which the quantity of solute in the gas varies from one end of the tower to the other while the solvent gas quantity does not. Treybal derived equations to relate composition change to mass transfer resistance and degree of condensation for the limiting cases of all diffusional resistance in the gas and all diffusional resistance in the liquid. Condensation of the solute was accounted for by dealing with the logarithmic average concentration of the non-diffusing solvent. This approach is only applicable for the case of single component transfer.

Kent and Pigford(4) considered a partial condenser fractionating device where condensation of both components from a binary vapor mixture occur simultaneously. Experimental studies of a condenser used to fractionate mixtures of ethylene dichloride and toluene showed that the observed mass transfer effects were in agreement with the Colburn-Drew(5) modification of Fick's Law. The Colburn-Drew theory reflects that the mass transfer rate of a component relative to stationary coordinates is the resultant of two effects: the transfer resulting from the bulk motion of the fluid and that resulting from the diffusion superimposed on the bulk flow. The authors apply this theory to Rayleigh's model, the material balance relationship for differential condensation, and derive new equations to relate composition change to mass transfer resistance, surface area and degree of condensation. Analytical equations are presented for the limiting cases of liquid phase and gas phase resistance alone. Integration by finite differences was required for the general case when both resistances are present.

II. THEORY

The usual technique for determining the degree of separation on an actual distillation plate involves predicting the Murphree vapor point efficiency $[E_{OG} = (y_2'-y_1)/mx_w-y_1)]$ from mass transfer units. The overall degree of plate separation expressed as the Murphree vapor plate efficiency $[E_{MV} = (y_2-y_1)/(mx_2-y_1)]$ is then predicted as a function of E_{OG}, mixing parameters which are based on plate geometry, rates and system physical properties. The presently used relationships for predicting E_{OG} and E_{MV} have been derived on the assumption that there is no net condensation or vaporization on a plate. In this section, equations are developed relating the degree of separation to degree of condensation, or vaporization, in addition to mass transfer resistance and mixing parameters.

The procedure used in developing the new equations parallels the derivation of the constant molal flow equations for determining Murphree vapor efficiencies. An equation is derived for predicting separation at a point on a distillation plate analogous to Murphree's(1) point efficiency equation except that the effects of flow between phases are included by applying the Colburn-Drew(5) theory. This theory reflects that the mass transfer rate of a component relative to stationary coordinates is the result of two effects: the transfer resulting from the bulk motion of the fluid and that resulting from the diffusion superimposed on the bulk flow. Finally, an equation is derived to determine the overall tray separation using the point degree of separation equation, mixing parameters and the degree of condensation or vaporization. This derivation is analogous to the AIChE eddy diffusion derivation(7) with the exception that non-constant molal flow was considered.

A FORTRAN program is presented in Appendix B for solving the final equations.

Derivation of Point Degree of Separation Equation

The development of equations for interphase mass transfer in distillation have generally been based on Whitman's(9) two film theory; i.e., resistance to mass transfer lies in parallel laminar fluid films between the phases. The assumptions inherent in this type of analysis are: (a) the rate of diffusional mass transfer of a component within a phase is proportional to the rate of change of concentration with distance at any point between the bulk phase and the interface; (b) equilibrium exists between phases at the interface; (c) the holdup of transferring components in the boundary layers is negligible with respect to the amount transferred in the process; and (d) the interface offers no resistance to mass transfer.

The following diagram illustrates a two film concentration profile for the case of mass transfer from vapor to liquid.

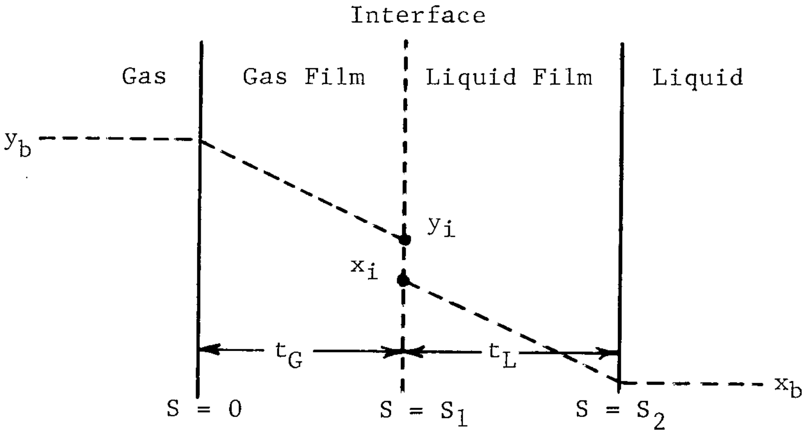

To derive the point separation equation the two film theory was applied to vertical slabs of differential length along the plate. As is done in the two film Murphree point efficiency case, it was assumed that the liquid concentration along vertical slabs is fixed and the composition of the vapor to the plate is homogeneous. Murphree's assumption of constant molal flow was replaced with the assumption that condensation or vaporization occurs linearly; i.e., the rate of change of vapor rate ($\triangle$) in the vertical direction is the same along all horizontal planes and the vapor rate (G) is fixed along any given horizontal plane. Thus, one model represents all vertical slabs along the plate and, as in the Murphree point efficiency case, the equation of point separation in a vertical slab is equivalent to the equation obtained for the entire tray when the liquid is completely mixed. This tray model is illustrated below:

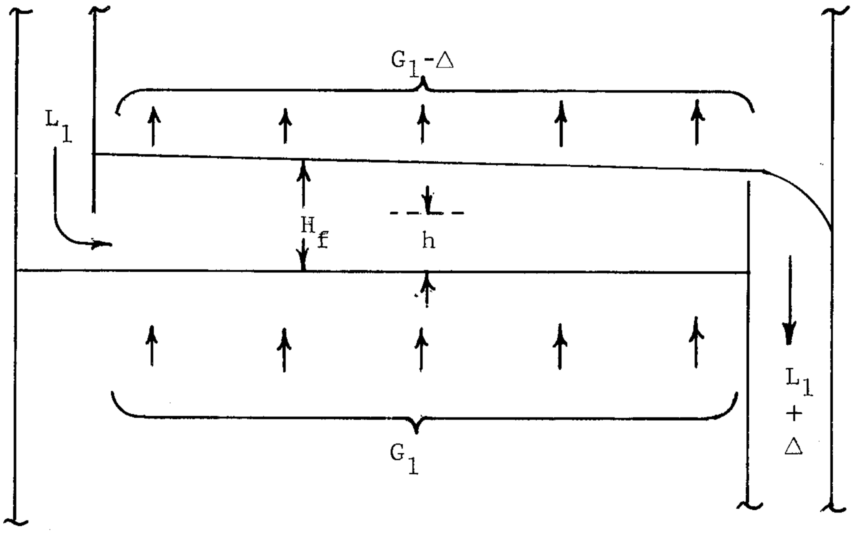

Point Separation Tray Model

Following are the derivations of the point separation equations for a completely mixed tray in the non-constant molal flow case and, for comparison, the conventional constant molal flow case.

A
Non-constant Molal Flow

B
Constant Molal Flow

- Application of Colburn-Drew(5) modification of Fick's Law to Gas Phase Mass Transfer

$$R_G = \left(\frac{-D_G P A_i dh}{RT\ H_f}\right)\left(\frac{dy}{dS}\right) + y\left(\frac{-dG}{dh}\right)dh \qquad (1A)$$

Where: $\frac{-dG}{dh} = \frac{\Delta}{H_f}$ for linear condensation and $\frac{D_G A_i}{RTt_G A_T H_f} = k_G a$ which, by definition, is the gas phase mass transfer coefficient. Substituting in (1A) gives:

$$R_G = -\left(k_G a A_T P t_G dh\right)\left(\frac{dy}{dS}\right) + y\left(\frac{\Delta}{H_f}\right) dh \qquad (2A)$$

$$R_G = \left(\frac{-D_G P A_i dh}{RT\ H_f}\right)\left(\frac{dy}{dS}\right) + 0 \qquad (1B)$$

Where: $\frac{D_G A_i}{RTt_G A_T H_f} = k_G a$ which, by definition, is the gas phase mass transfer coefficient. Substituting in (1B) gives:

$$R_G = -\left(k_G a A_T P t_G dh\right)\left(\frac{dy}{dS}\right) \qquad (2B)$$

- Integrating with respect to (S) at Steady State and Constant (h)

At steady state $\frac{dR}{dS} = 0$ and therefore:

$$\frac{d\left[-\left(k_G a A_T P t_G dh\right)\left(\frac{dy}{dS}\right) + y\left(\frac{\triangle}{H_f}\right)dh\right]}{dS} = 0 \quad (3A)$$

Integrating gives:

$$R_G = \left(-k_G a A_T P t_G dh\right)\frac{dy}{dS} + y\left(\frac{\triangle}{H_f}\right)dh = C_1 \quad (4A)$$

Integrating again:

$$\ell n\left[\left(\frac{\triangle}{H_f}\right)ydh - C_1\right] - \frac{\triangle}{k_G a A_T H_f P t_G} S = C_2 \quad (5A)$$

Where C_1 and C_2 are integration constants.

At steady state $\frac{dR}{dS} = 0$ and therefore:

$$\frac{d\left[-\left(k_G a A_T P t_G dh\right)\left(\frac{dy}{dS}\right)\right]}{dS} = 0 \quad (3B)$$

Integrating gives:

$$R_G = -\left(k_G a A_T P t_G dh\right)\left(\frac{dy}{dS}\right) = C_1' \quad (4B)$$

Integrating again:

$$\left(-k_G a A_T P t_G dh\right) y - C_1' S = C_2' \quad (5B)$$

Where C_1' and C_2' are integration constants.

- Insertion of Boundary Conditions

BC(1) $y=y_b$ @ $S=S_o$

BC(2) $y=y_i$ @ $S=S_1$

Where: $S_1 - S_o = t_G$

Solving for integration constants by applying boundary conditions to (4A) gives:

$$R_G = \left(\frac{\triangle}{H_f}\right)dh \frac{\left(y_i - y_b e^{\frac{\triangle}{GN_G}}\right)}{1 - e^{\frac{\triangle}{GN_G}}} = C_1 \quad (6A)$$

Where $N_G = k_G a P A_T H_f / G$ = gas mass transfer units by definition.

BC(1) $y=y_b$ @ $S=S_o$

BC(2) $y=y_i$ @ $S=S_1$

Where: $S_1 - S_o = t_G$

Solving for integration constants by applying boundary conditions to (4B) gives:

$$R_G = \frac{N_G G dh}{H_f}(y_b - y_i) = C_1' \quad (6B)$$

Where $N_G = k_G a P A_T H_f / G$ = gas mass transfer units by definition.

- Analogous Liquid Film Mass Transfer Equation

By analogy to Equation 6A:

$$R_L = \left(\frac{\Delta}{H_f}\right) dh \, \frac{\left(x_b - x_i e^{\frac{\Delta}{LN_L}}\right)}{1 - e^{\frac{\Delta}{LN_L}}} \qquad (7A)$$

Where $N_L = k_L \bar{a} \rho_L A_T H_f / L$ = liquid mass transfer units by definition, and $x_i = y_i/m$.

By analogy to Equation 6B:

$$R_L = \left(\frac{LN_L}{H_f}\right) dh \left(x_i - x_b\right. \qquad (7B)$$

Where $N_L = k_L \bar{a} \rho_L A_T H_f / L$ = liquid mass transfer units by definition, and $x_i = y_i/m$.

- Overall Mass Transfer Equation

By material balance $R_0 = R_L = R_G$.

Now by definition:

$$R_0 = \left(\frac{\Delta}{H_f}\right) dh \, \frac{\left(y^* - b_2 y_b\right)}{b_1 - b_2} \qquad (8A)$$

Where: $y^* = mx$ and b_1 and b_2 are arbitrary constants.

Now equating Equations 6A, 7A, and 8A, and solving for b_1 and b_2 gives:

$$b_1 = m + (1-m) e^{\frac{\Delta}{LN_L}} \qquad (9A1)$$

$$b_2 = \left(e^{\frac{\Delta}{GN_G}}\right)\left(e^{\frac{\Delta}{LN_L}}\right) \qquad (9A2)$$

By material balance $R_0 = R_L = R_G$.

Now by definition:

$$R_0 = \frac{N_{OG} \, G dh}{H_f} \left(y_b - y^*\right) \qquad (8B)$$

Where: $y^* = mx$ and N_{OG} = overall mass transfer units by definition.

Now equating Equations 6B, 7B, and 8B, and solving for N_{OG} gives:

$$\frac{1}{N_{OG}} = \frac{1}{N_G} + \frac{m \frac{G}{L}}{N_L} \qquad (9B)$$

Integration of Mass Transfer Equation With Respect To (h)

By material balance at height h on the plate:

$$R_0 = \frac{d\left(-Gy_b\right)}{dh}dh = -G\left(\frac{dy_b}{dh}\right)dh - y_b\left(\frac{dG}{dh}\right)dh \qquad (10A)$$

Equating 10A to 8A and substituting $-\frac{dG}{dh}$ back for $\frac{\triangle}{H_f}$ gives:

$$\frac{dy_b}{y^*-b_1y_b} = \frac{dG}{(b_1-b_2)G} \qquad (11A)$$

Integrating from $y_b=y_1$ to y_2' and $G=G_1$ to G_2 gives:

$$\frac{y^*-b_1y_2'}{y^*-b_1y_1} = e^{\left(\frac{b_1}{b_2-b_1}\right)\ln\frac{G_2}{G_1}} \qquad (12A)$$

By material balance at height h on the plate:

$$R_0 = \frac{d\left(-Gy_b\right)}{dh}dh = -G\left(\frac{dy_b}{dh}\right)dh \qquad (10B)$$

Equating 10B to 8B gives:

$$\frac{d_{yb}}{y^*-y_b} = -\frac{N_{OG}}{H_f}\,dh \qquad (11B)$$

Integrating from $y_b=y_1$ to y_2' and $h = 0$ to $h = H_f$ gives:

$$\frac{y^*-y_2'}{y^*-y_1} = e^{-N_{OG}} \qquad (12B)$$

Final Point Separation Equation

Rearranging 12A gives:

$$\frac{y_2'-y_1}{\frac{y^*}{b_1}-y_1} = 1-e^{\left(\frac{b_1}{b_2-b_1}\right)\ln\frac{G_2}{G_1}} \qquad (13A)$$

$E^* = \dfrac{y_2'-y_1}{\frac{y^*}{b_1}-y_1}$ by definition.

Rearranging 12B gives:

$$\frac{y_2'-y_1}{y^*-y_1} = 1-e^{-N_{OG}} \qquad (13B)$$

$E_{OG} = \dfrac{y_2'-y_1}{y^*-y_1}$ by definition.

The new equation for the non-constant molal flow case expresses the degree of separation at a point on a distillation tray as a function of the mass transfer terms ($N_G \cdot G$ and $N_L \cdot L$), the equilibrium constant (m), and the entering and leaving vapor rates (G_1 and G_2). It seems reasonable to assume that $N_G \cdot G$ and $N_L \cdot L$ values predicted from conventional correlations would be usable providing we use averages of the entering and leaving vapor and liquid rates in the prediction. Predicted leaving vapor and liquid compositions from the non-constant molal flow equations approach those of the constant molal flow equation as rate of condensation ($\triangle$) approaches zero (see Appendix D). The final non-constant molal flow point separation equation is summarized below:

$$E^* = \frac{y_2' - y_1}{\frac{y^*}{b_1} - y_1} = 1 - e^{\left(\frac{b_1}{b_1 - b_2}\right) \ell n \frac{G_1}{G_2}} \tag{13A}$$

Where: $b_1 = m + (1-m)\, e^{\frac{\triangle}{LN_L}}$

$$b_2 = \left(e^{\frac{\triangle}{GN_G}}\right)\left(e^{\frac{\triangle}{LN_L}}\right)$$

It should be noted that, unlike E_{OG}, E^* is <u>not</u> an efficiency and can thus be greater than 1 or negative in value.

An interesting phenomena arising from having net condensation or vaporization is that it is possible to have an equilibrium line cross on a perfectly mixed tray. An equilibrium line cross in a tray composition balance can be expressed analytically as a situation where y_{in}/x_{in} is $>$ than the tray equilibrium constant (m) with $y_{out}/x_{out} < m$ or $y_{in}/x_{in} < m$ and $y_{out}/x_{out} > m$. In the constant molal flow situation it is not possible to have an equilibrium line cross on a perfectly mixed tray, since this would imply a Murphree vapor point efficiency greater than 100%.

The reason it is possible to have an equilibrium line cross in the non-constant molal flow case is that a change in stream rates produces a corresponding change in stream compositions that is not dependent on equilibrium. The following example illustrates an equilibrium cross-situation on a perfectly mixed tray. The leaving compositions for this example were calculated using Equation-13A with $N_G = .5$, $N_L = .5$ and $m = 5$. As can be seen $[y_{in}/x_{in} = 10] > [m = 5]$ while $[y_{out}/x_{out} = 3.5] < [m = 5]$.

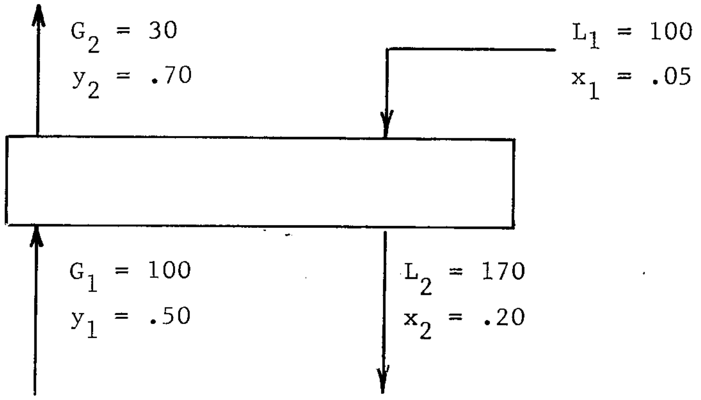

Derivation of Plate Degree of Separation Equation

As mentioned previously, if the liquid on a distillation plate was completely mixed the point degree of separation equation would express the degree of separation for the total streams leaving the plate. Practically, however, incomplete mixing is the norm and thus there is a need to be able to calculate overall plate separation as a function of the point separation equation and mixing parameters.

Anderson(6), Gerster et al(7), and Rukinshtein(8) have all separately derived a plate separation prediction equation using the concept of continuous mixing on the plate. In their model, recommended by the AIChE(7), the mixing streams are determined by the product of the concentration gradient in the froth and the eddy diffusity, with constant molal flow being assumed. This eddy diffusion model is rederived below on a non-constant molal flow basis. The point separation equation derived above is used in this derivation along with its inherent assumption of linear condensation, or vaporization; i.e., the rate of change of vapor rate in the vertical direction is the same along all horizontal planes and the vapor rate is fixed along any given horizontal plane. The analogous constant molal flow equations are not included because they are too complex to be of comparative value.

Consider the finite element of liquid shown on the plate segment below. The width of the element is equal to the width of the plate, the height is equal to the plate liquid froth height (H_f) and the element length is the differential length along the tray (dZ).

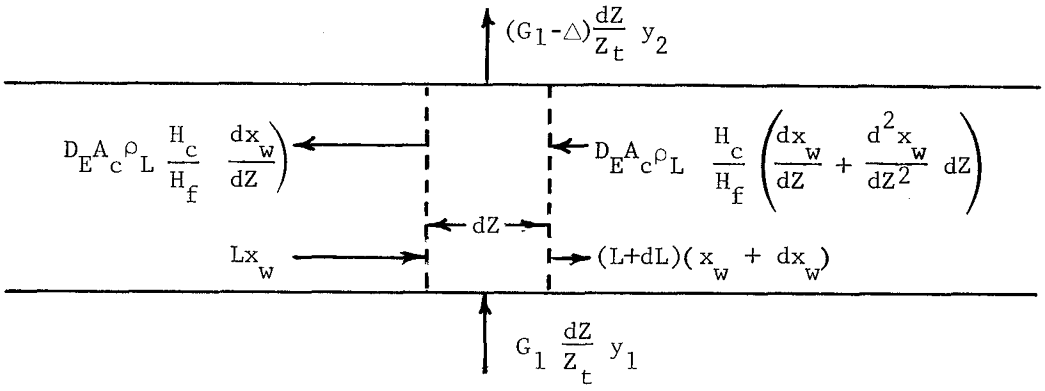

- Setup of Differential Equation

At steady state, a material balance around the differential liquid element gives:

$$y_1 G_1 \frac{dZ}{Z_t} + Lx_w + D_E A_c \rho_L \frac{H_c}{H_f}\left(\frac{dx_w}{dZ} + \frac{d^2x_w}{dZ^2}dZ\right)$$

$$= y_2 (G_1-\Delta)\frac{dZ}{Z_t} + (L+dL)\left(x_w + \frac{dx_w}{dZ}dZ\right) + D_E A_c \rho_L \frac{H_c}{H_f}\frac{dx_w}{dZ} \qquad (14)$$

Now substituting in the following relationships:

$\frac{Z}{Z_t} = w$ (By Definition)

$dL = \frac{\Delta}{Z_t}dZ$ and $L = L_1 + \frac{Z}{Z_t}\Delta$ (For Linear Condensation)

$\frac{y_2'-y_1}{y^*_{b_1} - y_1} = E^*$ (Point Separation Equation)

Solving with the dL.dx cross-product neglected, gives the following final differential equation:

$$\frac{d^2x_w}{dw^2} - \frac{Z_t\left(L_1+w\triangle\right)}{D_E A_c \rho_L \frac{H_c}{H_f}}\left(\frac{dx_w}{dw}\right) - \frac{Z_t\left[\frac{mE^*}{b_1}\left(G_1-\triangle\right)+\triangle\right]x_w}{D_E A_c \rho_L \frac{H_c}{H_f}} + \frac{y_1\left[E^*\ G_1+(1-E^*)\triangle\right]Z_t}{D_E A_c \rho_L \frac{H_c}{H_f}} = 0 \qquad (15)$$

- Integration of Differential Equation

Integrating by the Taylor series technique gives:

$$x_w = a_o\left(1+\frac{C_1}{2!}w^2+\frac{C_1C_2w^3}{3!}+\ldots\right)+a_1\left(w+\frac{C_2w^2}{2!}+\frac{\left(C_2{}^2+C_1+C_3\right)w^3}{3!}+\ldots\right)$$
$$-\ y_1\ C_4\left(\frac{w^2}{2!}+\frac{C_2w^3}{3!}+\frac{\left(C_2{}^2+2C_3+C_1\right)w^4}{4!}+\ldots\right) \qquad (16)$$

Where: $C_1 = \frac{Z_t}{D_E A_c \rho_L \frac{H_c}{H_f}}\left[\frac{mE^*}{b_1}\ (G_2)+\triangle\right]$

$C_2 = \frac{Z_t L_1}{D_E A_c \rho_L \frac{H_c}{H_f}}$

$C_3 = \frac{Z_t \triangle}{D_E A_c \rho_L \frac{H_c}{H_f}}$

$C_4 = \frac{Z_t}{D_E A_c \rho_L \frac{H_c}{H_f}}\left[E^*\ G_1+(1-E^*)\ \triangle\right]$

a_o and a_1 = integration constants

- Insertion of Boundary Conditions:

B.C.1 @ w=0 $\qquad x_{w=0} = x_1 + \left(\frac{D_E A_c \rho_L \frac{H_c}{H_f}}{Z_t L_1} = \frac{1}{C_2}\right)\left(\frac{dx_w}{dw}\right)_{w=0}$

B.C.2 @ w=1 $\qquad \frac{dx_w}{dw} = 0$

Solving for a_o and a_1 at boundary limits gives:

$$a_o = \frac{y_1 C_4 \left[1 + \frac{C_2}{2!} + \frac{C_2{}^2 + 2C_3 + C_1}{3!} + \ldots\right] + x_1 C_2 \left[1 + C_2 + \frac{C_2{}^2 + C_1 + C_3}{2!} + \ldots\right]}{\left[C_1 + \frac{C_1 C_2}{2!} + \frac{C_1 C_2{}^2 + 2C_1 C_3 + C_1{}^2}{3!} + \ldots\right] + C_2 \left[1 + C_2 + \frac{C_2{}^2 + C_1 + C_3}{2!} + \ldots\right]} \qquad (17)$$

$$a_1 = (a_o - x_1)\, C_2$$

- Final integrated equation:

Inserting a_o and a_1 functions into the integrated equation and rearranging gives the following final equation for x_w:

$$x_w = (T_1 + 1)\, T_5 + (T_5 - x_1)\, C_2 T_2 - T_1 \frac{C_4}{C_1} y_1 \qquad (18)$$

Where: C_1, C_2, C_3, C_4 are the groups defined in Equation-16 and the T terms are series expressions defined below:

$$\begin{array}{lllll}
 & i=1 & i=2 & i=3 & i=i \\
T_1 = & 0 + & \frac{C_1}{2!} w^2 + & \frac{C_1 C_2}{3!} w^3 & + \frac{\alpha_i w^i}{i!} \\
T_2 = & w + & \frac{C_2 w^2}{2!} + & \frac{C_1 + C_3 + C_2{}^2}{3!} w^3 & + \frac{\alpha_i w^i}{i!} \\
T_3 = & 0 + & C_1 + & \frac{C_1 C_2}{2!} & + \frac{\alpha_i}{(i-1)!} \\
T_4 = & 1 + & C_2 + & \frac{C_1 + C_3 + C_2{}^2}{2!} & + \frac{\alpha_i}{(i-1)!}
\end{array}$$

With $\alpha_i = \alpha_{i-2} \left[C_1 + C_3(i-2)\right] + \alpha_{i-1} (C_2)$

$$T_5 = \frac{\left(y_1 T_3 \frac{C_4}{C_1} + C_2 T_4 x_1\right)}{\left(T_3 + C_2 T_4\right)}$$

The non-constant molal flow Equation-18 expresses the liquid composition (x_w) at any point along the flow path length of a distillation plate as a function of inlet stream compositions (y_1 and x_1), the point separation Equation-13A, mixing parameters based on plate geometry, and the plate overall stream material balance. To determine a plate's leaving liquid composition, solve the equation at $w = 1.0$. The average leaving vapor composition is, of course, determinable by material balance. Composition predictions from this equation approach the point separation Equation-13A predictions as eddy diffusivity approaches infinity. The authors have written and debugged a FORTRAN program for solving the new equations and this program is presented in Appendix B. At constant molal flow, predictions are in agreement, ±0.3% with the conventional constant molal flow Equation-Ap9 (see comparison in Appendix B).

III. EXPERIMENTAL PROCEDURE

Description of Apparatus

The apparatus used in this investigation was constructed by the authors. It consisted of a six inch I.D. bubble cap plate distillation column (see Figures 1 and 2) with a reboiler and condenser. The column was constructed of twc single cap, cast glass, plates flanged between twelve inch "Pyrex" sections. The reboiler was a large "Pyrex" flask that was flanged to the column. The charge capacity of the reboiler was approximately seven gallons. The condenser was a double pipe exchanger fabricated from galvanized iron pipe. Steam tracing and insulation were used to minimize system heat losses. Heat was supplied by an electric resistance heater and removed by cooling water. The system was vented to the atmosphere. To prevent combustible vapors from contacting the heater elements, continuous purging by air was used. Pressure protection was assured by a 1 atmosphere gauge rupture disc.

Thermometers were located at the following points:

(1) Vapor space between the reboiler and bottom plate
(2) Bottom plate
(3) Vapor space between the bottom and top plates
(4) Top plate
(5) Vapor stream entering the condenser
(6) Reflux to the top plate
(7) Cooling water leaving the condenser

Samples were taken at the points indicated on Figure 1. They were as follows:

(1) Reflux line to the top plate

(2) Mid-point on the top plate

(3) Mid-point on the bottom plate

A pressure gauge was located at the top of the tower.

Reflux rates were measured by means of a rotameter placed in the reflux return line. The system was designed such that gravity return reflux could be maintained.

Experimental Procedure

The experimental procedure consisted primarily of observing top plate compositions at varying reflux composition and temperature. Measurements were recorded for reflux rate; tower temperatures; top pressure; reflux, top plate and bottom plate compositions. Before the runs were initiated, the system was tested with methanol. This served two purposes; first to locate leaks and second to clean the system. The system was thoroughly air dried before admitting the toluene charge. It was found that the reagent grade toluene contained sufficient water to bring the reflux close to saturation for the low temperature runs of the investigation. For the high temperature runs, which were executed last, water was added to the system.

In executing a run the cooling water to the condenser, the reboiler heating coils and the insulation steam tracing were turned on and the tower allowed to heat up. Throughout the procedure, the column was run at total reflux. Flow in the system started approximately after one-half hour. Lining out of the cold reflux runs took approximately an additional hour. The hot reflux runs took approximately an additional two hours. During this time, temperatures and flow rates were observed to find out if the system was approaching steady state. In addition, the sampling lines were periodically purged to minimize contamination from previous sampling and/or free water depositing from cooling in stagnant areas. Samples, approximately equal to 50 ml in volume, were taken and the temperatures, reflux rate and pressure noted. Samples were withdrawn slowly to be sure "point" samples were obtained.

Analysis

The weight of water in the samples was determined by titration using the Karl Fischer Reagent technique. The method is based on the following reaction(10).

$$I_2 + SO_2 + H_2O + 3C_5H_5N + CH_3OH \rightarrow 2C_5H_5N\bullet HI + C_5H_5N\bullet HSO_4CH_3$$

Precautions were taken to prevent contamination by absorbed and/or adsorbed water in the samples, Karl Fischer reagent and analytical equipment. Flasks and pipettes were oven dried until use was required. The burette assembly contained a drying tube. Care was taken in admitting samples so that eddying of air into the titration flash was kept at a minimum. Samples containing high concentrations of water that hazed when cooled down to room temperature were carefully reheated to redissolve precipitated water.

The concentration of water in the toluene samples was found in the following manner. The samples were drained from the column into oven dried 75 ml flasks. The sample flasks were covered with plastic stoppers while transporting from the laboratory to the analysis room to prevent contamination from atmospheric water vapor. The samples were then transferred from the sample flasks to the titrating flasks by means of oven dried 50 ml pipettes.

Standard Karl Fischer reagent was used for the analysis. The reagent was standardized before use against an accurately measured quantity of a standard water in methanol solution. One milliliter of the standard contained one milligram of water. The end points achieved in titration of the standard were within ±0.05 ml. The end points attained in the titration of the samples were felt to be within the same range.

Figure 1

DISTILLATION COLUMN

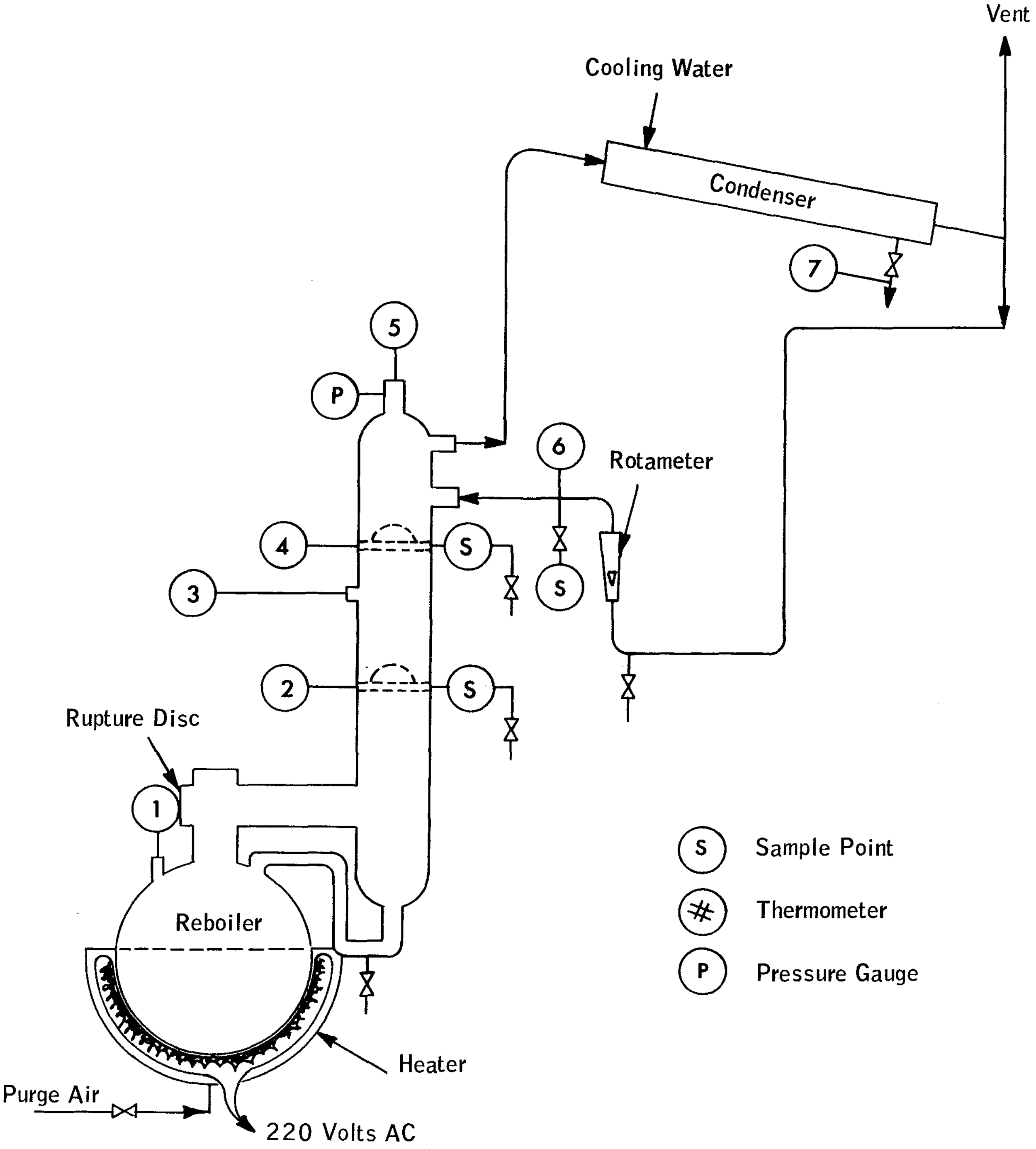

Figure 2

TRAY DETAILS

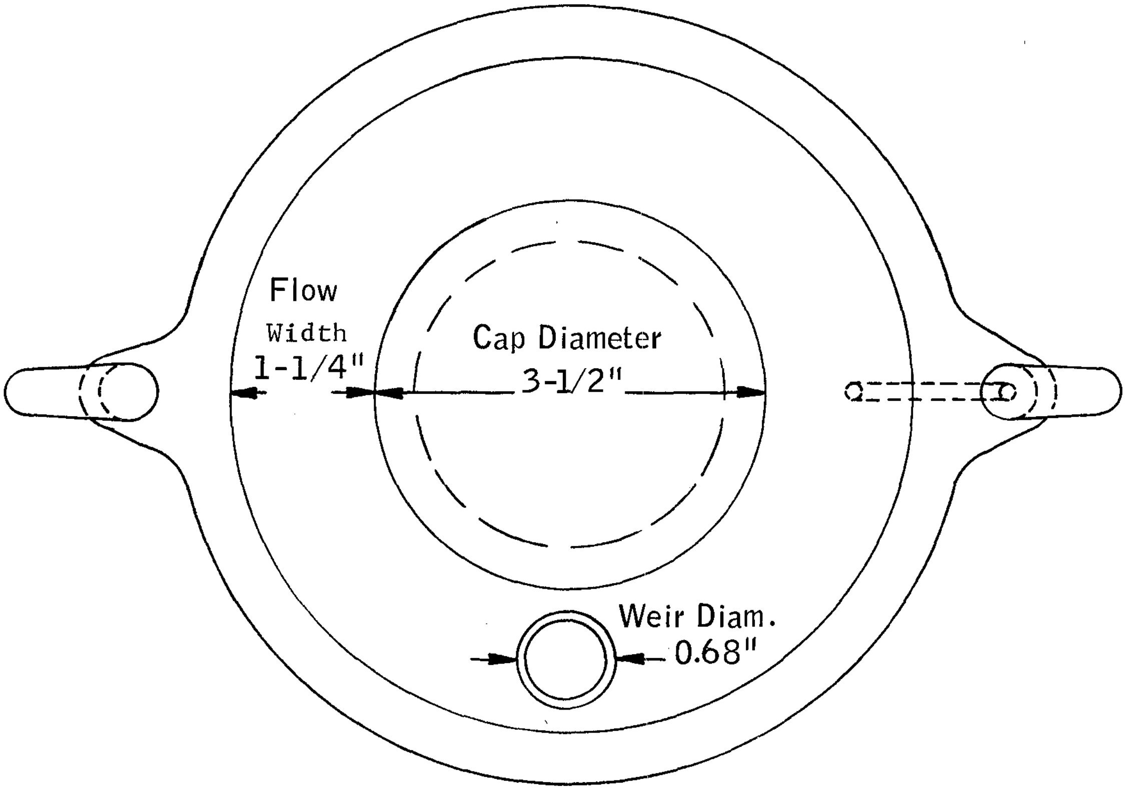

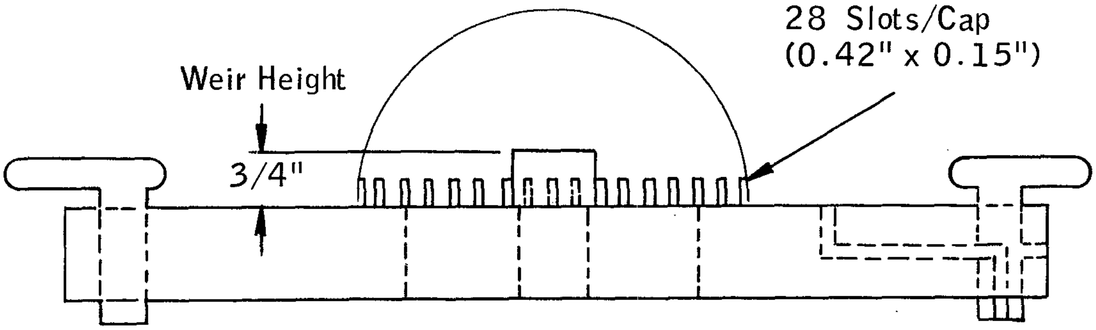

IV. EXPERIMENTAL DATA

The attached tables present the measurements data taken during the course of this experiment. The symbols referred to in the tables are defined below:

X-A - wppm of water in liquid to top tray
X-B - wppm of water in liquid at middle of top tray
X-C - wppm of water in liquid at middle of bottom tray
T-1 - °F, temperature of liquid to top tray
T-2 - °F, temperature of vapor off top tray
T-3 - °F, temperature of top tray
T-4 - °F, temperature of vapor off bottom tray
T-5 - °F, temperature of bottom tray
T-6 - °F, temperature of vapor from reboiler
R - %, reading on reflux rotameter
P - psig, tower top pressure
Hf - inches, froth height on top plate

Figure 1, Page 21 shows the exact location of these various measurement points.

TABLE I
EXPERIMENTAL RUNS DATA

Run	Date 1965	X-A wppm	X-B wppm	T-1 °F	T-2 °F	T-3 °F	T-4 °F	T-5 °F	T-6 °F	R, %	P, psig	Top Tray Hf, inches
1	6/12	13.3	133	80	231	222	234	225	240	12.5	0	(1)
2	6/17	24.4	295	80	231	222	234	225	238	12.5	0	(1)
3	6/20	25.5	308	82	231	222	234	226	249	12.5	0	(1)
4	6/27	23.0	289	82	231	222	234	226	249	12.5	0	(1)
5	6/27	13.3	146	85	231	222	234	226	249	13.0	0	(1)
6	7/2	47.8	694	165	231	223	232	225	249	16.0	0	(1)
7	7/7	41.0	497	163	231	224	232	225	234	19.0	0	(1)
8	7/7	49.0	523	172	231	224	233	225	234	17.0	0	(1)
9	7/8	40.0	493	165	231	224	233	225	234	17.5	0	(1)
10	7/8	72.0	953	159	231	224	234	225	238	16.0	0	(1)
11	7/9	64.5	1065	166	231	224	233	225	239	16.5	0	(1)
12	7/14	47.5	650	121	231	223	233	225	237	14.5	0	(1)
13	7/15	49.0	700	119	231	223	233	220	245	14.5	0	(1)
14	7/28	56.5	705	118	231	223	232	225	234	14.5	0	(1)
15	7/29	33.4	500	178	231	223	232	225	234	16.5	0	(1)
16	7/31	45.5	866	189	231	223	233	225	241	17.0	0	(1)
17	7/31	38.0	522	107	231	222	233	225	236	13.0	0	(1)
18	7/31	32.0	510	108	231	222	233	225	238	13.0	0	(1)
19	7/31	30.0	482	109	231	222	233	225	238	13.0	0	(1)
20	7/31	35.5	460	100	231	222	233	225	238	13.0	0	(1)
21	8/11	30.0	278	206	231	224	233	225	234	18.0	0	(1)
22	8/14	53.4	605	193	231	224	232	225	236	17.5	0	(1)
23	8/14	86.0	1830	176	231	224	232	225	236	17.0	0	(1)
24	8/14	72.0	1110	185	231	224	233	225	240	17.0	0	(1)
25	8/14	53.0	1110	185	231	224	233	225	241	17.0	0	(1)

Note (1) - Top tray froth height was measured at 1.10 inches for T-1 = 110°F. No visual change in froth height could be seen from run-to-run.

TABLE II
BOTTOM PLATE ANALYSES (X-C)

Date 1965	X-C wppm
6/3	7.1
6/5	14.0
6/12	15.5
6/27	25.0

V. DISCUSSION OF EXPERIMENTAL RESULTS

Development of Predictions for Comparison to Data

The plate separation Equation-18 presented on Page 18 is a general expression for liquid composition, x_w, at any point along a distillation plate as a function of: inlet stream compositions (y_1 and x_1), the point separation Equation-13A, mixing parameters and the entering and leaving stream rates. In this experiment a two plate tower was run at total reflux and because of this Equation-18 can be simplified. Starting with Equation-18 at w = 1 and substituting the total reflux conditions of $y_1 = x_2$ and $y_2 = x_1$ the following is obtained:

$$\frac{y_2}{x_2} = \frac{\left[T_1' \frac{C_4}{C_1} + 1\right]\left[T_3 + C_2 T_4\right] - T_3 \frac{C_4}{C_1}\left[T_1' + 1 + C_2 T_2'\right]}{C_2\left[(T_1'+1)\ T_4 - T_2'\ T_3\right]} = T_6 \qquad (19)$$

where T_1' and T_2' are the values of T_1 and T_2 at w = 1

Thus an expression (T_6) for y_2/x_2, the ratio of leaving vapor and liquid compositions, is obtained as a function of the T and C terms.

As mentioned in the Experimental Procedure Section III, this work consisted primarily of measuring top plate compositions at varying reflux composition and temperature. As mentioned above, since the tower was at total reflux, the reflux composition x_1 was equal to the top plate leaving vapor composition y_2. The top plate liquid composition measured, however, was taken from a tap located in the middle of the plate and thus was <u>not</u>

equal to x_2. (The plate was not modified to permit taking outlet samples, since it became evident early in the experiment that outlet compositions, x_2, were below the practical limits of analysis, e.g., less than 5 wppm.) Therefore, Equation-19 cannot be used directly. However, substituting $T_6 = \frac{y_2}{x_2} = \frac{x_1}{y_1}$, into Equation-18 the following relationship between y_2 and x_w is obtained:

$$\frac{y_2}{x_w} = \frac{1}{\left[\left(T_1+1+C_2T_2\right)\left(\frac{C_4}{C_1}\right)\left(\frac{T_3}{T_3+C_2T_4}\right) - \frac{T_1C_4}{C_1}\right]\frac{1}{T_6} - \left[T_2 - \frac{T_4\left(T_1+1\right) + C_2T_2T_4}{T_3+C_2T_4}\right]C_2} \qquad (20)$$

The T terms in Equation-20 are all related to C terms, see Page 18, and the C's are groupings of predictable system values, see Page 17. These system values are all composition independent and thus $y_2/x_{w=.5}$ is composition independent. The only parameter intentionally varied from run to run, besides concentration, was the temperature of the liquid to the top plate, i.e., the reflux temperature. Thus, composition data from the system should be plotted as $y_2/x_{w=.5}$, i.e., y_{out}/x_{mid}, versus reflux temperature. In order to compare these data with the new theoretical model, y_{out}/x_{mid} as a function of reflux temperature was predicted using Equation-20. This equation along with Equations 18 and 19 was solved by the FORTRAN program of Appendix B. The estimation of the system values, at each reflux temperature, required as input for the program will now be considered.

In predicting system values the vapor rate to the top plate was assumed constant in all runs. This vapor rate was determined by making heat balances around the top plate for each run using the recorded reflux temperature and the rotameter reading converted into reflux rate as per Appendix E. An average vapor rate of 0.783 lb moles/hr was calculated with values ranging from .737 to 0.847 lb moles/hr. Most of this deviation appeared to be due to inaccuracies in reading the reflux rotameter since tower heat input was held constant.

Another assumption made was that the liquid on the top plate was at the temperature of the vapor leaving the plate, i.e., 231°F. (The vapor temperature approximates the boiling point of toluene, 231.2°F, since the water concentrations in the system are far too low to have an effect on temperatures.) Although the thermometer reading for the top plate read 222-224°F, this was corrected up to 231°F since the same thermometer read 225°F for the bottom plate where the temperature was obviously 231°F. The low reading is explained by the thermometer being in the plate, not in the liquid, and thus measuring plate instead of liquid temperature.

The sample calculation, presented in Appendix C, outlines stepwise how the system values were calculated for a specific reflux temperature. The relationships used in these calculations, and the reasons for their use, are outlined below:

(1) Gas Diffusivity - The Slattery-Bird(11) equation was used for gas diffusivity on the basis of its being specifically applicable for the binary system of water in a non-polar gas at low pressure.

(2) Liquid Diffusivity - The Wilke(12) equation was used for liquid diffusivity, since it is usually good within ±10% for dilute solutions of non-dissociating solutes.

(3) Equilibrium Constant - Calculated from Henry's Law using water vapor pressure, and solubility in toluene data.

(4) Gas and liquid mass transfer units - The relationships for gas (N_G) and liquid (N_L) mass transfer units given in the AIChE University of Michigan report(13) on tray efficiencies in distillation columns were used. These relationships were selected on the basis that the report included more data on small column operations than other available sources. A spot-check of the Michigan predictions against the AIChE design manual method(7) gave consistent results.

(5) Froth and Clear Liquid Heights - The following equation for clear liquid height (H_c) was derived herein by assuming Gester's(7) equation (H_c, inches = 0.19 W + 1.65 - .65F + .02 Lgpm) could be applied in the form (K - .65F + .02 Lgpm). To determine K, the measured froth height of 1.10 inches at a reflux temperature = 110°F and H_c/H_f = .58 from the AIChE Michigan report(13) Figures 4-27, Page 19, were used. The equation derived for this experiment is:

$$H_c = .825 - .65F + .0226\ L_{mph} \qquad (21)$$

where L is the average of entering and leaving liquid rates.

This equation in conjunction with the Michigan H_c/H_f correlation Figure 4-27 were used for predicting H_c and H_f values at varying reflux temperatures.

(6) Eddy Diffusivity - An absolute value of the eddy diffusivity (D_E) could not be reliably predicted since there are no data available in the low range of vapor and liquid rates of this experiment. Referring to the AIChE Delaware(7) report, Gilbert's(14) work and the correlations developed by Barker and Self(15), predicted D_E's range from negative values up to a maximum of 26. The absolute value of D_E is not critical in this experiment since the interest is primarily in the change in separation rather than in the absolute magnitude of the separation. A middle of predictions D_E was selected, $D_E = 12$, and this gave y/x's in the data range. This value was taken as constant with varying reflux temperature since plate froth height, the correlating parameter for D_E, was observed and calculated to be essentially constant across the experimental reflux temperature range.

Curve I Figure 3 is the plot of y_{out}/x_{mid} versus reflux temperature predicted by running the computer program (Appendix B) with system values predicted as outlined above. For comparison, Curve II presents a constant molal flow approximation prediction. Curve II was obtained by taking the same system values as for Curve I but using the conventional Murphree point efficiency Equation-13A for point separation and the Appendix B program with rate of condensation = 0, and average vapor and liquid rates to get overall plate separation. Curve I shows an increase of 18% in y_{out}/x_{mid} when decreasing temperature across the experimental reflux temperature range of 205 to 80°F, as compared to a 10% increase for Curve II. These curves would be even further apart except for the compensating effects of the point separation Equation-13A and the new mixing Equation-18. This compensation is discussed in detail in the "Discussion of Theory Section."

Correction to Basic Data To Account for Contamination

Due to the low concentrations of water present in the plate samples, especially the low reflux temperature runs, it was evident that contamination would have a significant effect on the data. The presence of contamination is clearly indicated by comparison of the middle of top plate water concentrations (Table 1, Page 27) to that of the bottom plate (Table 2, Page 28). As indicated, these concentrations are close in value. One would have expected the bottom concentrations to be less than 1 wppm on the basis of theoretical predictions. On occasion, bottom plate compositions were so high (on days of high humidity) that operation of the distillation column was terminated with no runs being made. Because of this source of error, the following technique was used to correct the basic data to account for contamination.

In theory, at a single reflux temperature, if the vapor compositions (y_{out}) from the top plate are plotted against the middle of the top plate liquid compositions (x_{mid}) and extrapolated, the intersection of this extrapolation with the $y_{out} = x_{mid}$ line defines the contamination level (k^*). The assumption of constant level of contamination is made here. This is shown by the following illustration, where the measured compositions yield line L_1.

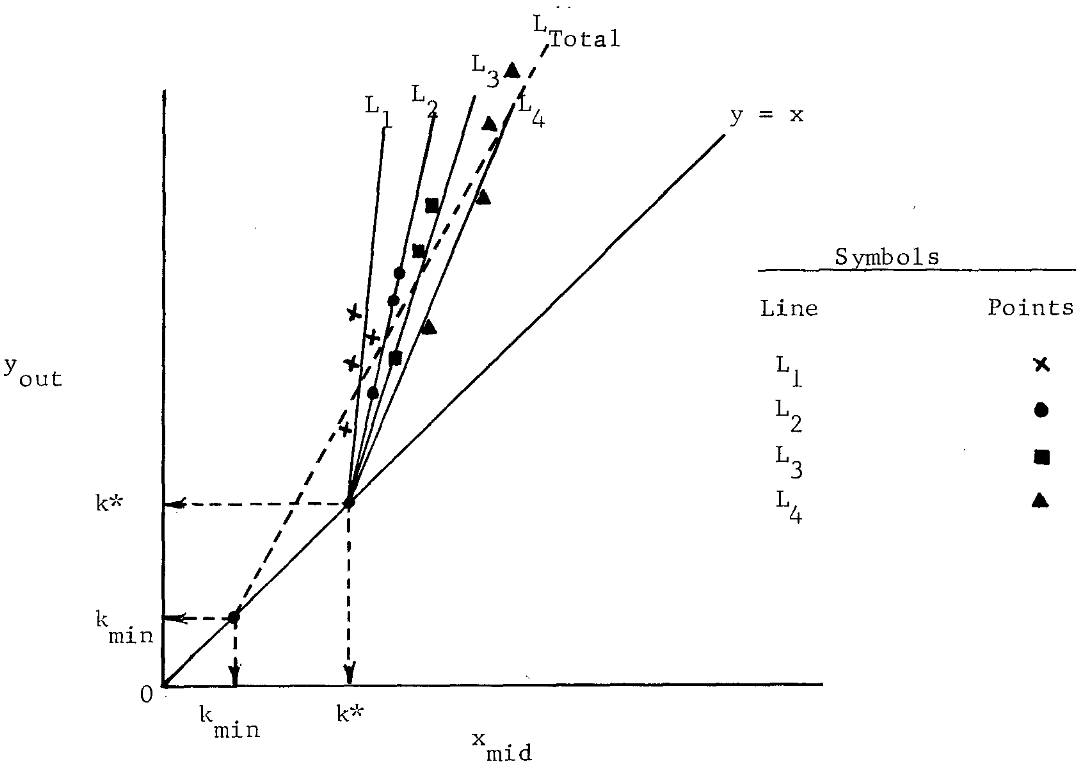

Similarly, compositions taken at increasingly higher temperatures should yield characteristic lines (L_2, L_3 and L_4) intersecting at the same point. The slopes of these lines are theoretically equal to the y_{out}/x_{mid} values shown in Curve I Figure 3. As can be seen from Curve I, the higher the reflux temperature, the lower the value of y_{out}/x_{mid} and therefore the flatter the slope of the y vs. x line. Since none of the groups of points corresponding to the various reflux temperatures were sufficient to draw separate y vs. x lines, all the points were used in drawing a single line; i.e., line L_{Total} on the above sketch.

The points taken were usually higher in concentration at higher temperatures, essentially patterning as shown on the sketch. Since the grouping of points were connected along lines of descending slope, as is shown qualitatively, the level predicted (k_{min}) is less than the actual value (k^*). The quantitative evaluation of (k_{min}) is shown on Figure 4. A value of 12 wppm H_2O was estimated for (k_{min}) by regression analysis.

Verification of the estimated value for the contamination level was obtained by comparison with measured bottom plate compositions. The average of bottom plate concentrations was 15 wppm H_2O. Since the true contamination level should be higher than the 12 wppm estimated level, and since the true bottom plate concentration should be less than 1 wppm H_2O, a contamination level of 15 wppm H_2O was subtracted from the data. Because of this subtraction, two of runs (Nos. 1 and 5) were deleted from the basic data workup (measured concentrations less than 15 wppm H_2O).

As mentioned earlier, moisture in the air was expected to be the major source of sample contamination. Since the sample containers were carefully dried by heating in an oven before use, the most obvious source of error appeared to be in the transference of the sample to the titration flask. The net volume of the flask before admitting the sample was 150 CC; after adding the sample it was 100 CC. A considerable amount of air might have been circulated into the flask while the sample was being added, perhaps more than 50 CC. A calculation was made to determine the extent to which the sample could be contaminated from this source. The following conditions were assumed as the basis for this calculation: Air admitted = 50 CC; temp. = 80°F; relative humidity = 70%, sample size being titrated = 50 CC. On the basis of this data, it was estimated that the contamination level from this source could be as high as 20 wppm H_2O. Since the contamination level calculated was greater than those estimated and measured it would appear that reasonable care was taken to minimize eddying of air into the titration flask and the 15 wppm assumed as the average contamination level is not unreasonably high.

It is interesting to note that previous investigations on water-hydrocarbon efficiency, Pickle's(17) M. S. thesis on water in benzene and toluene and Gester's(18) commercial data on water in hexane, reported lower efficiencies than would be predicted. The data used in these investigations do not appear to be corrected for contamination and this may be the reason for the lower than expected efficiencies.

Comparison of Data and Predictions

The corrected composition data, plotted as y_{out}/x_{mid} versus reflux temperature, are shown on Figure 5. Regression of these data with all points equally weighted yielded Curve A. As can be seen there is considerable scatter of the data around Curve A. This scatter is a result of the extreme sensitivity of y_{out}/x_{mid} to composition errors. The error in doing a titration could easily be $\pm$.05 CC of reagent, the equivalent of $\approx \pm 5$ wppm. A variation of +5 wppm in y_{out} with - 5 wppm in x_{mid} for points below the line, or -5 wppm in y_{out} with +5 wppm in x_{mid} for points above the line, is more than sufficient to return most of the points to the line. Because of this extreme sensitivity the data were regressed on a weighted basis giving more credit to those data points which were made at higher y and x values and thus are less sensitive to error.

As a weighting factor $\frac{x_{mid}, \text{wppm} - 5}{x_{mid}, \text{wppm}}$ was used. Curve B, Figure 5, is the result of this weighted regression analysis.

Curve A, with the points equally weighted show a 42% increase of y_{out}/x_{mid}, when decreasing temperature across the experiment temperature range of 205 to 80°F, while Curve B shows a 22% increase. This range of 42% to 22% should now be compared to the 18% increase predicted by the non-constant molal flow model, Curve I, Figure 3, and the 10% increase predicted by the constant molal flow approximation case, Curve II, Figure 3. Because of the closeness of the two predictions, the data plots cannot be used to show up the difference between the two types of models. What can be said is that the data exhibit a definite trend in the direction predicted by the new model, i.e., increasing y_{out}/x_{mid} with decreasing reflux temperature. The magnitude of this trend is reasonably close to the new model prediction when considered in the light of possible experimental error.

Figure 3

THEORETICAL Y_{OUT}/X_{MID} PREDICTIONS

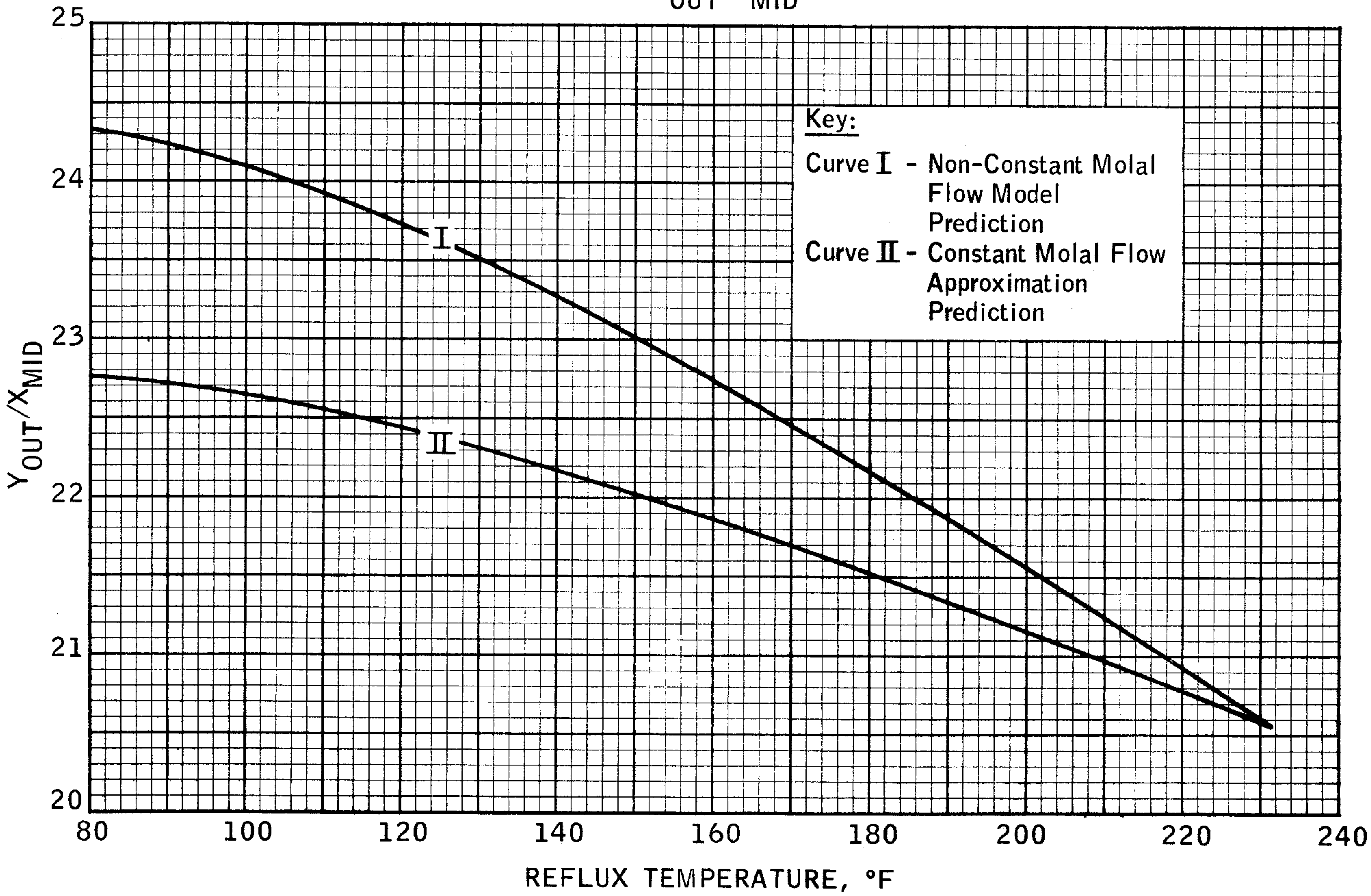

Figure 4

PLOT OF Y_{OUT} VS X_{MID} DATA

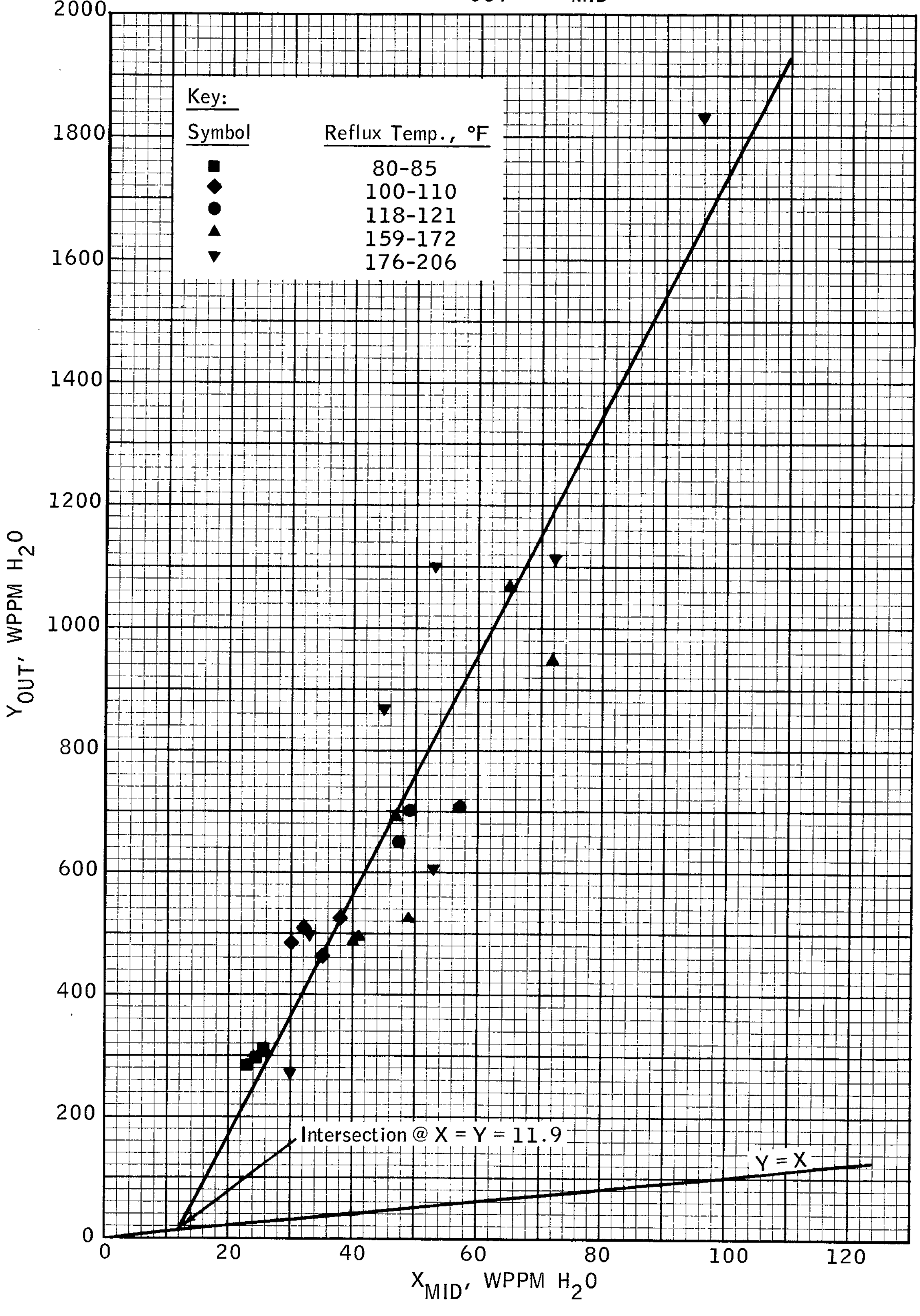

Figure 5

PLOT OF CONTAMINATION CORRECTED DATA, $(Y_{OUT}-15)/(X_{OUT}-15)$

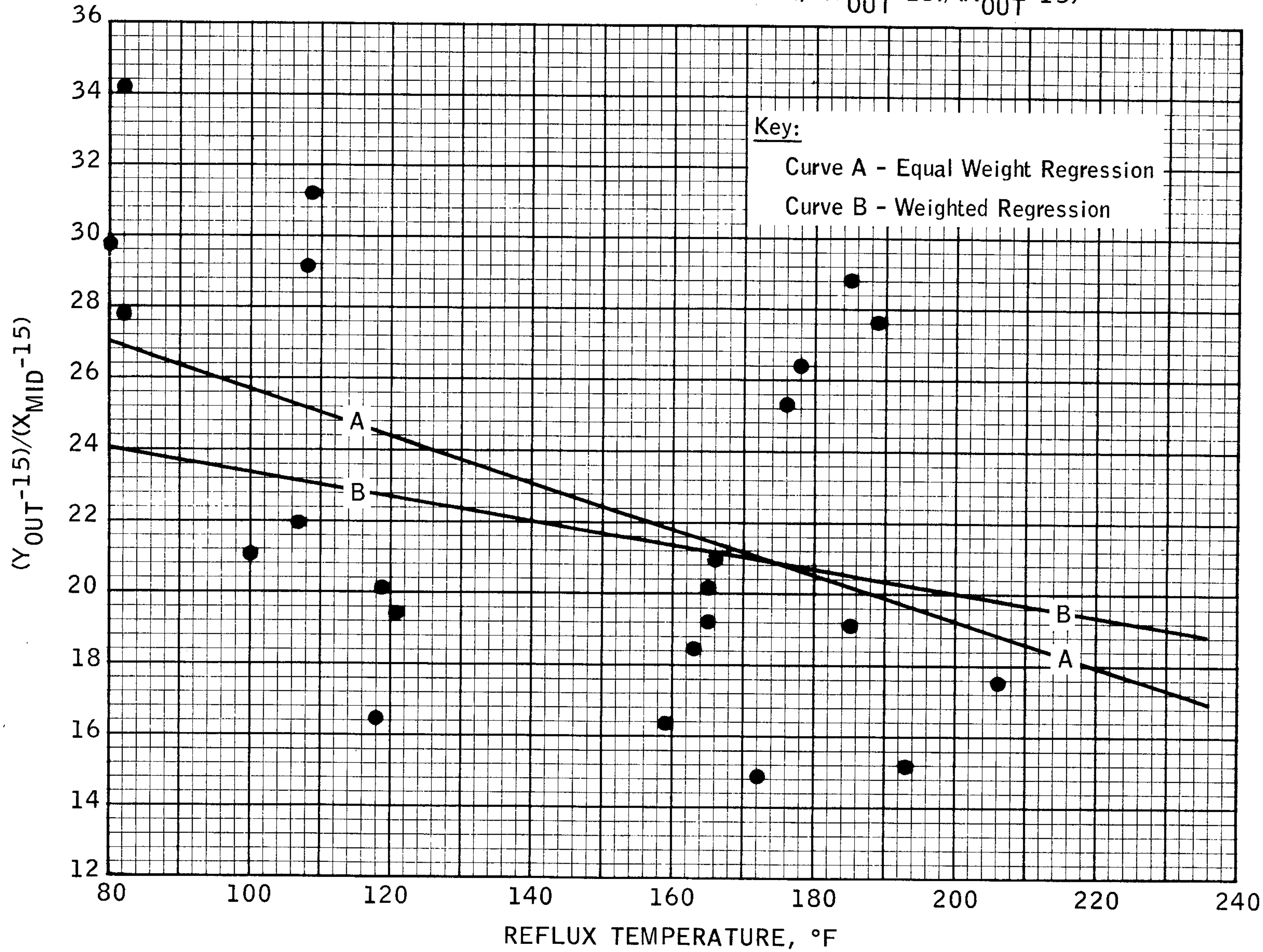

VI. DISCUSSION OF THEORY

The equations developed in Section II relate the degree of separation on a distillation plate to degree of condensation, or vaporization, in addition to mass transfer resistances and mixing parameters. Condensation and evaporation were brought in by assuming these effects occur linearly; i.e., the rate of change of vapor rate with vertical distance is the same along all horizontal planes and the vapor rate is fixed along any given horizontal plane. To bring into account the actual fashion in which vapor rate varies horizontally and vertically would require bringing into account the energy transfer, in addition to mass transfer, relationships. To do this one would need heat transfer coefficient data of which there are very little available. In addition, the relationships involved would be of an order of magnitude more complicated than the relationships presented here.

Another simplification which will normally have to be made in applying the theoretical equations of Section II is that the temperatures of the vapor and liquid leaving the tray are equal. Accounting for leaving stream temperature differences would require having heat transfer coefficient data.

What remains to be considered is how the predictions by the new relationships compare with using the present constant molal flow relationships for the non-constant molal flow case. As described in Section II, the effects of condensation and vaporization were brought into account by first rederiving Murphree's point separation equation and then rederiving the AIChE eddy diffusivity model for overall plate separation. The effects of these corrections are illustrated for this thesis experiment by Figure 6. Curve 1 is the predicted plot of y_{out}/x_{out} versus reflux temperature, obtained by using the new point separation equation and new eddy diffusivity model, and Curve 2 is the predicted plot obtained by using the average of inlet and outlet rates in the constant molal flow relationships. The curves are fairly close together and y_{out}/x_{out} is higher in the constant molal flow approximation case. The closeness of the two curves is, however, a result of the compensating effects of the point separation correction and the eddy diffusivity model correction. This is illustrated by Curve 3 which is a plot obtained using the new point separation equation but with the constant molal flow approximation for the eddy diffusivity model. Curve 3 y_{out}/x_{out} values are much higher than those of Curve 2. Thus, for this thesis experiment it was important to take into account both corrections.

The compensating nature of the point separation equation and the eddy diffusivity model corrections cannot be considered typical of what would happen in other systems. More often, one can expect the point separation equation correction to be more important. The correction to the eddy diffusivity model was comparable to the point separation correction for this experiment due to the importance of non-mixing effects at the unusually high stripping factor $\left(\frac{mG}{L}\right)$ ratio , $\frac{mG}{L} = 43.5$. The unmixed, plug flow, y_{out}/x_{out} for $\frac{mG}{L} = 43.5$ would be 4700 as compared to $y_{out}/x_{out} \approx 10$ for the perfectly mixed case.

Figure 6

PREDICTED Y_{OUT}/X_{OUT} VS REFLUX TEMPERATURE

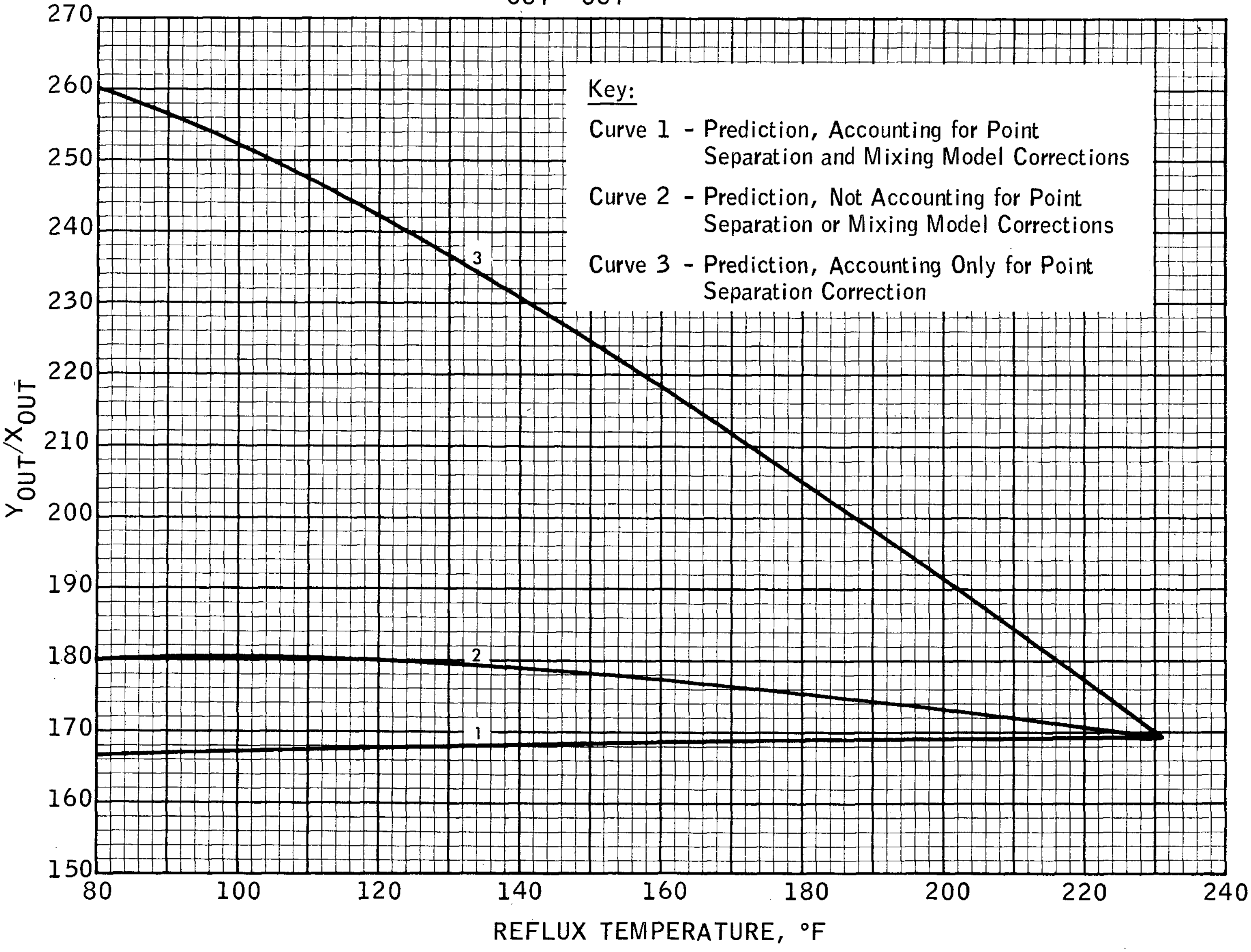

Key:

Curve 1 - Prediction, Accounting for Point Separation and Mixing Model Corrections

Curve 2 - Prediction, Not Accounting for Point Separation or Mixing Model Corrections

Curve 3 - Prediction, Accounting Only for Point Separation Correction

VII. CONCLUSIONS AND RECOMMENDATIONS

The following conclusions can be drawn:

1. The new point and plate degree of separation equations that have been developed offer a means for determining the effect of non-constant molal flow upon the actual separation achieved on a distillation plate. Thus, they go one step further than the existing AIChE(7) equations which were derived assuming constant molal flow. That the new equations are theoretically sound is demonstrated by the excellent agreement with the AIChE equations when solved for the condition of constant molal flow.

2. Conclusive proof on the validity of the new equations could not be drawn from the data taken on the system water-toluene. However, the data did exhibit a definite trend in the direction predicted by the new equations.

3. Study of partially miscible systems dealing with analysis of low concentrations of water requires sophisticated sampling and analytical techniques to minimize effects of sample contamination. This was evident in this work in that a contamination level of about 15 wppm water was exhibited by the data. Also, the Karl Fischer method is not an adequate technique for the determination of water at the concentration levels used in this work. This was substantiated by the effect that the ±5 wppm titration accuracy had on the least squares regression of the data.

It is recommended that the following investigations be considered for future work:

1. Study additional systems that exhibit low efficiency to verify the model proposed in this work. Systems such as acetone-water and isopropanol-water exhibit point efficiencies in the range of 50 to 70%. These systems are also completely miscible over all concentration levels, thus permitting experiments that would minimize the effects of contamination and analytical inaccuracy.

2. Use the new separation equations to prepare mixing curves similar to those prepared by the AIChE(7) for E_{MV}/E_{OG} as a function of N_{Pe}, E_{OG}, and mG/L. It is envisioned that the proposed mixing curves would relate E^*_{Plate}/E^*_{Point} as a function of N_{Pe}, $\triangle/L_1$ E^*_{Point} and G_{avg}/L_{avg}.

3. Investigate and apply the new separation equations by physically incorporating them into a plate-to-plate calculation procedure. In this manner, the sensitivity of fractionation to variations in separation efficiency due to deviations in molal overflow can be investigated. The Theile-Geddes procedure using the "vaporization efficiency" concept as explained by Holland(21) can be readily adapted to utilize the new separation equations.

VIII. APPENDIX

TABLE OF CONTENTS

APPENDIX SECTION A
NOMENCLATURE

$a, \bar{a}$ - interfacial area, sq. ft./cu. ft. of tray holdup.

A_i - interfacial area on tray, sq. ft.

A_T - active cross-sectional area of tray perpendicular to gas, sq. ft.

A_C - cross-sectional area of liquid flow on tray, sq. ft.

b_1, b_2 - constants defined in point separation Equation-13A.

C_1, C_2, C_3, C_4 - constants defined in plate separation Equation-18.

D_E - eddy diffusivity, sq. ft/hr.

D_G - gas diffusivity, sq. ft./hr.

D_L - liquid diffusivity, sq. ft./hr.

E_{MV} - Murphree vapor plate efficiency.

E_{OG} - Murphree vapor point efficiency.

E^* - composition change term defined in point separation Equation-13A, unitless.

G - vapor rate passing up through tray, lb. moles/hr.

G_1, G_2 - vapor rate to and from tray, respectively, lb. moles/hr.

h - vertical height off base of tray, feet.

H_c - clear liquid height on tray, cu. ft./sq. ft.

H_f - froth height on tray, feet.

k_G - gas phase mass transfer coefficient, lb. moles/sq. ft-hr-atm.

$k_G a$ - gas phase mass transfer coefficient, lb. moles/cu. ft-hr-atm.

k_L - liquid phase mass transfer coefficient, ft./hr.

$k_L \bar{a}$ - liquid phase mass transfer coefficient, hr^{-1}.

K_{OG} - overall gas phase mass transfer coefficient, lb. moles/sq. ft-hr-atm.

$K_{OG}a$ - overall gas phase mass transfer coefficient, lb. moles/ft.^{3}-hr-atm.

L - liquid rate along flow path length of tray, lb. moles/hr.

L_1, L_2 - liquid rate to and from tray, respectively, lb. moles/hr.

m - slope of the vapor-liquid y vs. x equilibrium curve.

N_G - number of gas phase mass transfer units, unitless.

N_L - number of liquid phase mass transfer units, unitless.

N_{OG} - number of overall gas phase mass transfer units, unitless.

P - total pressure above tray, atmospheres.

Q - stream enthalpy, Btu's/lb. mole.

R - universal gas constant, cu. ft.-atm./°R-lb. moles.

R_o - overall mass transfer of component between bulk vapor and bulk liquid at height h, lb. moles/hr.

R_G - mass transfer of component out of bulk vapor at height h, lb. moles/hr.

R_L - mass transfer of component into bulk liquid at height h, lb. moles/hr.

S - distance along films between bulk vapor and bulk liquid, feet.

t_G, t_L - thickness of pseudo-laminar gas and liquid films, feet.

$T°$ - temperature, degree scale specified where used.

V_s - superficial velocity of vapor to plate, ft./sec.

w - fractional length along tray liquid flow path, unitless.

W_t - width of liquid flow path, feet.

x_b - bulk liquid concentration in tray segment, mole fraction.

x_i - liquid concentration at gas/liquid interface in tray segment at height h, mole fraction.

x_w - liquid concentration at point w along flow path length of tray, mole fraction.

x_o - liquid concentration on tray at w = 0, mole fraction.

x_1 - concentration of liquid to tray, mole fraction.

x_2 - concentration of liquid from tray, mole fraction.

y_b - bulk vapor concentration in tray segment at height h, mole fraction.

y_i - vapor concentration at gas-liquid interface in tray segment at height h, mole fraction.

y^* - equilibrium vapor concentration = $m\ x_b$, mole fraction.

y_1 - concentration of vapor to tray, mole fraction.

y'_2 - local concentration of vapor leaving tray at point w, mole fraction.

y_2 - average concentration of vapor leaving tray, mole fraction.

Z - distance along flow path length of tray, feet.

Z_t - total flow path length of tray, feet.

Greek Symbols

Δ - (G_1-G_2) = rate of condensation on tray (negative for vaporization), lb. moles/hr.

ρ_G - vapor density, lbs./cu. ft.

ρ_L - liquid density, lbs./cu. ft.

ρ_{LM} - liquid molal density, lb. moles/cu. ft.

μ_L - liquid viscosity, lb.-mass/ft.-hr.

θ_L - liquid residence time, seconds.

APPENDIX SECTION B
FORTRAN PROGRAM

Solution of the new plate degree of separation equation was achieved by means of a series technique. As applied to our system, a high degree series expansion is required. The authors have written and debugged an IBM FORTRAN II program for solving the new point and plate degree of separation equations utilizing double precision arithmetic for accuracy.

In this section are:

(1) A simplified logic diagram
(2) Nomenclature defining the variables used in the program
(3) A detailed program listing

LOGIC DIAGRAM FOR EFFICIENCY PROGRAM

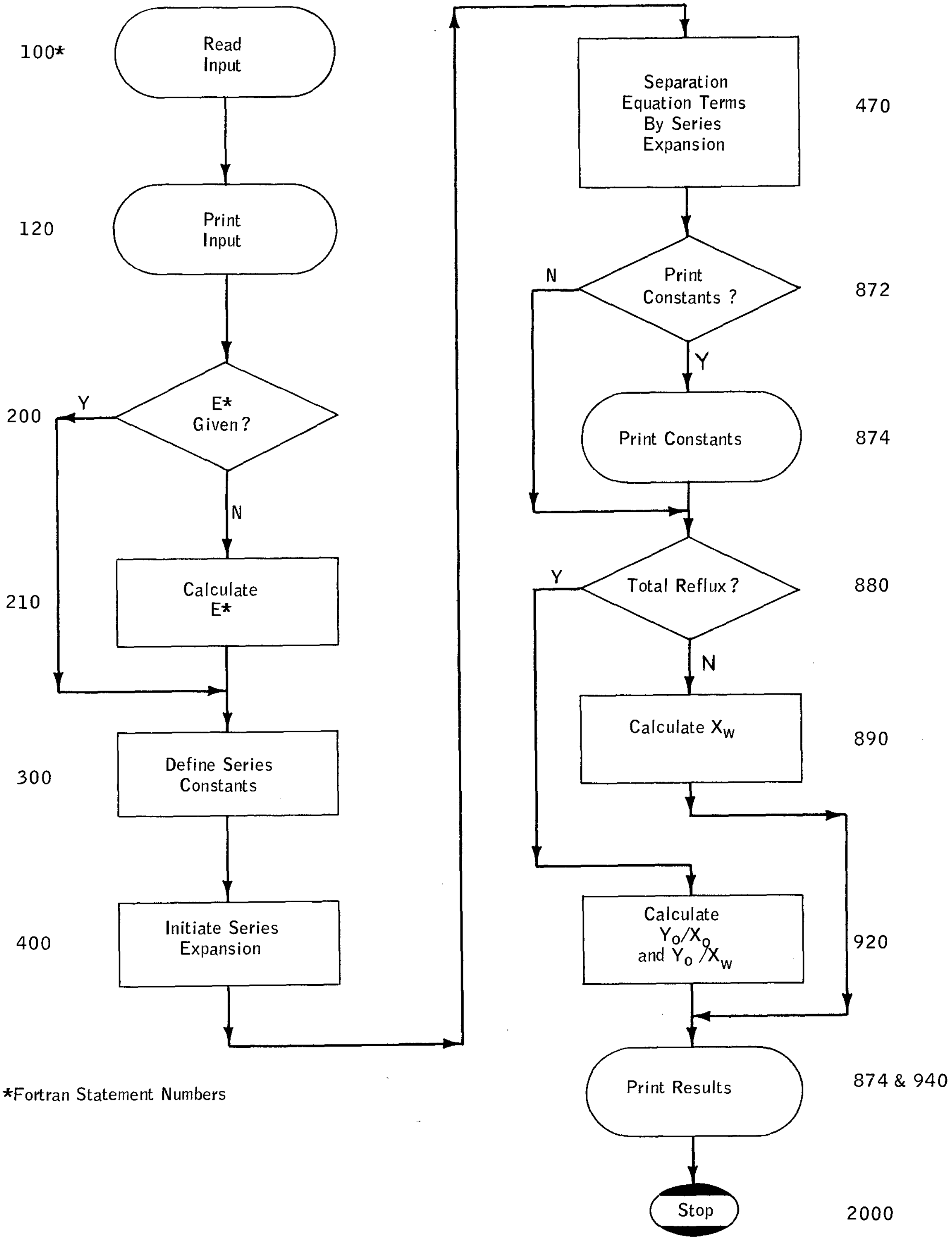

*Fortran Statement Numbers

MAIN PROGRAM NOMENCLATURE

A - A_c, cross-sectional area of liquid flow on tray, sq. ft.

A1 - $e^{\frac{\Delta}{GN_G}}$

A2 - $e^{\frac{\Delta}{LN_L}}$

ALPHA - Taylor series expansion terms

$$\left.\begin{array}{l}\text{B1 -}\\ \text{B2 -}\end{array}\right\} \text{Constants used in evaluating } E_{OG}$$

CASE - Case number

$$\left.\begin{array}{l}\text{C1 -}\\ \text{C2 -}\\ \text{C3 -}\\ \text{C4 -}\end{array}\right\} \text{Expansion constants as defined by Equation-18 in Theory Section}$$

DE - D_E, eddy diffusivity

DELTAL - Δ, rate of condensation

DIVIDE - Programming constant

ELAVG - $\left[L_1 \ (L_1+\Delta) \right]^{0.5}$

EL1 - L_1

EM - m, slope of equilibrium curve

ENG - N_G, gas mass transfer units

ENL - N_L, liquid mass transfer units

EOG - E^*, composition change term, defined in Equation 13A in Theory Section

FACT - Programming constant

G1 - G_1, vapor rate to tray

G2 - Constant used in evaluating y_2/x_2 and y_2/x_w

GAVG - $\left[G_1 \, (G_1 - \Delta) \right]^{0.5}$, geometric average of inlet and outlet vapor rates

IADD - Programming constant

NIXIT - Path control

RHOL - ρ_L, liquid density

RHOF - $\frac{H_c}{H_f}$, froth density

R1 -
R2 - Constants used in setting up C_1, C_2, C_3 and C_4
R3 -

SIGMA - Summation of Taylor series expansion

T1 -
T2 -
T3 - Expansion terms as defined by Equation-18 in Theory Section II
T4 -

TOL - Termination tolerance for Taylor series expansion

W - w, fractional distance along tray

X1 - x_1, inlet liquid concentration

XW - x_w, liquid composition at point w on tray

Y1 - y_1, inlet vapor composition

YOTX0T - y_2/x_2, outlet vapor composition/outlet liquid composition

YOTXW - y_2/x_w, outlet vapor composition/liquid composition at point w

Z1 - Z_t, total flow path length

SUBROUTINE EXPAND NOMENCLATURE

A - Used to test series expansion convergence

AI - An indexing variable

TERM - A term in the series expansion

Other constants defined the same as used in the Main Program.

```
C     EFFECT ØF DEVIATIØN FRØM CØNSTANT MØLAL ØVERFLØW ØN PLATE EFF.
C
C     BY - NIEDZWIECKI AND WEISSMAN
C
D     DIMENSIØN  ALPHA(200)
D     CØMMØN     ALPHA,C1,C2,C3,FACT,DIVIDE,IADD,SIGMA,W,TØL
C
C     INPUT
C
  100 READ 1000, CASE,Y1,X1,DE,RHØL,RHØF,Z1,A,G1,EL1
  110 READ 1000, DELTAL,W,EØG,EM,ENL,ENG,B1,TØL,PRINT
  115 PRINT 1115
  120 PRINT 1200, CASE,Y1,X1,DE,RHØL,RHØF,Z1,A,G1,EL1,DELTAL,W,EØG,EM,
     1           ENL,ENG,B1,TØL
C
C     PØINT EFFICIENCY FRØM NL AND NG
C
D 200 IF (EØG) 300,210,300
D 210 GAVG = SQRTF(G1*(G1 - DELTAL))
D 220 ELAVG = SQRTF(EL1*(EL1 + DELTAL))
D 230 A1 = EXPF(DELTAL/(ENG*GAVG))
D 240 A2 = EXPF(DELTAL/(ENL*ELAVG))
D 250 B1 = EM - A2*EM + A2
D 260 B2 = A1*A2
D 270 EØG = 1.0 - EXPF((B1/(B1 - B2))*LØGF(G1/(G1 - DELTAL)))
  280 PRINT 1280, EØG,B1
C
C     DEFINITIØN ØF CØNSTANTS
C
D 300 R1 = Z1/(DE*A*RHØL*RHØF)
D 310 R2 = EM*EØG*(G1 - DELTAL)/B1 + DELTAL
D 320 R3 = (EØG*G1) + (1.0 - EØG)*DELTAL
D 330 C1 = R1*R2
D 340 C2 = R1*EL1
D 350 C3 = R1*DELTAL
D 360 C4 = R1*R3
C
C     START ØF CALCULATIØN
C
  400 NIXIT = 0
D 410 IF (Y1) 420,420,470
D 420 WSET = W
D 430 W = 1.0
  440 GØ TØ 470
D 450 W = WSET
  460 NIXIT = 1
C
C     T1 DETERMINATIØN
C
D 470 ALPHA(1) = 0.0
D 480 ALPHA(2) = C1
D 490 SIGMA = 1.0 + 0.5*C1*(W**2)
D 500 FACT = 2.0
  510 IADD = 1
```

```
D 520 DIVIDE = 1.0
  530 CALL EXPAND
D 540 T1 = SIGMA
C
C     T2 DETERMINATIØN
C
D 550 ALPHA(1) = 1.0
D 560 ALPHA(2) = C2
D 570 SIGMA = W + 0.5*C2*(W**2)
D 580 FACT = 2.0
  590 CALL EXPAND
D 600 T2 = SIGMA
D 610 IF (Y1) 620,620,660
  620 IF(NIXIT) 630,630,660
D 630 T1P = T1
D 640 T2P = T2
  650 GØ TØ 450
  660 CØNTINUE
C
C     T3 DETERMINATIØN
C
D 730 ALPHA(1) = 0.0
D 740 ALPHA (2) = C1
D 750 SIGMA = C1
D 760 FACT = 1.0
D 765 DIVIDE = W
  770 IADD = 0
  780 CALL EXPAND
D 790 T3 = SIGMA
C
C     T4 DETERMINATIØN
C
D 800 ALPHA(1) = 1.0
D 810 ALPHA(2) = C2
D 820 SIGMA = 1.0 + C2
D 830 FACT = 1.0
  840 CALL EXPAND
D 850 T4 = SIGMA
C
C     EQUATIØN CØNSTANTS PRINTØUT
C
  872 IF (PRINT) 880,880,874
  874 PRINT 1874, R1,R2,R3,C1,C2,C3,C4
  876 PRINT 1876, T1,T2,T1P,T2P,T3,T4
C
D 880 IF (Y1) 920,920,890
C
C     EQUATIØN FØR NØN-TØTAL REFLUX
C
D 890 G1 = (Y1*T3*(C4/C1) + C2*T4*X1)/(T3 + C2*T4)
D 892 XW = G1*T1 + (G1 - X1)*C2*T2 - Y1*(T1 - 1.0)*(C4/C1)
  900 PRINT 1900, XW
  910 GØ TØ 2000
C
```

```
C     EQUATIØN FØR TØTAL REFLUX
C
D 920 G2 = T3 + C2*T4
D 934 YØTXØT = (((T1P - 1.0)*(C4/C1) + 1.0)*G2 - T3*(C4/C1)*
D    1          (T1P + C2*T2P))/(C2*(T4*T1P - T3*T2P))
D 935 YØTXW = 1.0/(((T1 + C2*T2)*(C4/C1)*(T3/G2) - (T1 - 1.0)*(C4/C1))*
D    1         (1.0/YØTXØT) - (T2 - (T4*T1 + C2*T2*T4)/G2)*C2)
  940 PRINT 1940, YØTXØT,YØTXW
C
C     FØRMATS
C
 1000 FØRMAT (10F7.2)
C
 1115 FØRMAT(1H1)
C
 1200 FØRMAT
     CASE NUMBER = @F0
      SPACE 2
     INPUT
      SPACE 1
          Y1      =         @E5
          X1      =         @E5
          DE      =         @E5
          RHØL    =         @E5
          RHØF    =         @E5
          Z1      =         @E5
          A       =         @E5
          G1      =         @E5
          EL1     =         @E5
          DELTAL  =         @E5
          W       =         @E5
          EØG     =         @E5
          EM      =         @E5
          ENL     =         @E5
          ENG     =         @E5
          B1      =         @E5
          TØL     =         @E5
      SPACE 2
     RESULTS
      SPACE 1
      END ØF FØRMAT
C
 1280 FØRMAT
          EØG     =         @E5
          B1      =         @E5
      SPACE 1
      END ØF FØRMAT
C
 1874 FØRMAT
     R1         R2            R3           C1           C2           C3
X     C4
         @E5          @E5          @E5          @E5          @E5          @E5
X         @E5
      SPACE 1
```

```
      END ØF FØRMAT
C
 1876 FØRMAT
     T1         T2          T1P         T2P          T3          T4
         @E5         @E5         @E5         @E5         @E5         @E5
      SPACE 1
      END ØF FØRMAT
C
 1900 FØRMAT
          XW     =         @E5
      SPACE 1
      END ØF FØRMAT
C
 1940 FØRMAT
          YØTXØT =         @E5
          YØTXW  =         @E5
      END ØF FØRMAT
C
 2000 CALL RETURN
      END
```

```
C
C     EVALUATIØN ØF PØWER SERIES
C
      SUBRØUTINE EXPAND
C
D     DIMENSIØN  ALPHA(200)
D     CØMMØN    ALPHA,C1,C2,C3,FACT,DIVIDE,IADD,SIGMA,W,TØL
C
  100 DØ 190 I = 3,200
D 110 AI = I
D 120 ALPHA(I) = ALPHA(I-2)*(C1 + (AI - 2.0)*C3) + C2*ALPHA(I-1)
D 130 AI = I - 1 + IADD
D 140 FACT = FACT*AI
D 150 TERM = ALPHA(I)*((W/DIVIDE)**AI)/FACT
D 160 SIGMA = SIGMA + TERM
D 170 A = TERM/SIGMA
D 171 IF (ALPHA(I) - 1.0E+30) 180,180,172
D 172 ALPHA(I) = ALPHA(I)*1.0E-20
D 174 ALPHA(I-1) = ALPHA(I-1)*1.0E-20
D 176 FACT = FACT*1.0E-20
  178 GØ TØ 190
D 180 IF (A - TØL) 220,220,190
  190 CØNTINUE
  210 PRINT 2100, I,ALPHA(I),SIGMA,A
  220 RETURN
C
C     FØRMATS
C
 2100 FØRMAT (10X,4HI = I3/10X11HALPHA(I) = E12.5/10X8HSIGMA = E12.5/10X
     14HA = E12.5)
C
      END
```

APPENDIX SECTION C
SAMPLE CALCULATION

Statement of the Problem

Predict y_2/x_2 ratio at total reflux for the following plate conditions. These are the conditions for one of the experimental runs of this thesis.

Plate conditions:

System - Water Dissolved in Toluene

Vapor Rate to Tray - 0.783 lb. moles/hour

Temperature of Vapor to Plate - 231°F

Temperature of Liquid to Plate - 80°F

Temperature of Liquid and Vapor Off Plate - 231°F

Total Pressure Above Plate - One Atm.

Active Cross-sectional Area of Plate (A_T) - 18.6 sq. inches

Width of Liquid Flow Path (W_t) - 2.5 inches

Liquid Flow Path Length (Z_t) - 7.45 inches

Solution of Problem

Step 1) Predict Physical Properties

a) Gas Diffusivity (D_G)

D_G is calculated via the Slattery-Bird(11) equation for H_2O in a non-polar gas at low pressure:

$$\frac{P\,D_G}{\left(P_{CA}\,P_{CB}\right)^{1/3}\left(T^\circ_{CA}\,T^\circ_{CB}\right)^{5/12}\left(\frac{1}{MA}+\frac{1}{MB}\right)^{1/2}} = a\left(\frac{T^\circ}{\sqrt{T^\circ_{CA}\,T^\circ_{CB}}}\right)^{b} \qquad (21)$$

$a = 3.64 \times 10^{-4}$, $b = 2.334$, $M_A = 18$, $M_B = 92.13$, $P = 1$ atm, $T = 383.8°K$,

$P_{CA} = 218.4$ atm, $P_{CB} = 41.6$ atm, $T_{CA} = 647.2°K$, $T_{CB} = 593.6°K$

$$\left(\frac{1}{M_A} + \frac{1}{M_B}\right)^{0.5} = \left(\frac{1}{18} + \frac{1}{92.13}\right)^{0.5} = 0.256$$

$$\sqrt{T^{\circ}_{CA} \cdot T^{\circ}_{CB}} = \sqrt{(647.2).(593.6)} = 620$$

$$\left(T^{\circ}_{CA} \cdot T^{\circ}_{CB}\right)^{5/12} = \left[(647.2)(593.6)\right]^{5/12} = 210$$

$$\left(P_{CA}\ P_{CB}\right)^{1/3} = \left[(218.4)(41.6)\right]^{1/3} = 20.8$$

$$\left(\frac{T^{\circ}}{\sqrt{T^{\circ}_{CA}\ T^{\circ}_{CB}}}\right)^{6} = \left(\frac{383.8}{620}\right)^{2.334} = 0.327$$

$$D_G = 3.64(10^{-4})(0.327)(0.256)(210)(20.8) = 0.133\ \text{cm}^2/\text{sec}$$

$$D_G\ \text{ft}^2/\text{hr} = \frac{.133(3600)}{6.45(144)} = 0.515\ \text{ft}^2/\text{hr}$$

b) Liquid Diffusivity (D_L)

D_L is calculated via the Wilke-Chang$^{(12)}$ equation for dilute solutions of non-dissociating solutes:

$$D_L = \frac{7.4(10^{-8})(\psi_B\ M_B)^{\frac{1}{2}}\ T^{\circ}}{\mu\ V_A 0.6}$$

$V_A = 18.8$ cm^3/g-mole, $\mu = 0.25$ centipoises, $\psi_B = 1.0$,

$M_B = 92.13$, $T = 383.8$ K

$$\left(\psi_B M_B\right)^{\frac{1}{2}} = (92.13)^{\frac{1}{2}} = 9.6$$

$$V_A^{0.6} = (18.8)^{0.6} = 5.78$$

$$D_L = \frac{7.4(10^{-8})(9.6)(383.8)}{(0.25)(5.78)} = 1.88 \times 10^{-4} \text{ cm}^2/\text{sec}$$

$$D_L(\text{ft}^2/\text{hr}) = 1.88 \times 10^{-4} \frac{(3600)}{6.45(144)} = 7.29 \times 10^{-4} \text{ ft}^2/\text{hr}$$

c) Equilibrium Constant

$$m = \frac{\text{Vapor pressure}}{\text{Total pressure x mole fraction solubility}}$$

Vapor pressure = 21.2 psia, Total pressure = 14.7 psia

Mole fraction solubility = 0.0332 - per Hibbard and Schalla(19)
at T = 231°F

$\therefore m = 43.5$

d) Bulk Stream Properties

The quantity of water dissolved in toluene at the conditions of this experiment is so minute, i.e. less than 0.10% wt percent, that the properties of toluene can be used to represent the entire stream. Maxwell's Data Book on Hydrocarbons(20) was used as a source of information for these properties.

$$\rho_{G_{231°F}} = \frac{M_w}{379} \times \frac{520}{T,\ °R} \times \frac{P,\ atm}{1} = \frac{92.13}{379} \times \frac{520}{692} \times \frac{1}{1} = 0.184 \text{ lbs/ft}^3$$

$$\rho_{L_{231°F}} = 48.6 \text{ lbs/ft}^3$$

$$\mu_{L_{231°F}} = .25 \text{ centipoises}$$

Step 2) Calculate Stream Rates by Heat Balance

$$G_1\, Q_{G_1} + L_1\, Q_{L_1} = G_2\, Q_{G_2} + L_2\, Q_{L_2}$$

$G_1 = L_2$ and $G_2 = L_1$ since tower at total reflux

$$\text{Then } \frac{G_2}{G_1} = \frac{Q_{G_1} - Q_{L_2}}{Q_{G_2} - Q_{L_1}}$$

$Q_{G_1} = Q_{G_2} = 29{,}400$ Btu /lb mole at $T = 231°F$

$Q_{L_1} = 8{,}750$ Btu /lb mole at $T = 80°F$

$Q_{L_2} = 15{,}050$ Btu /lb mole at $T = 231°F$

$$\therefore \quad \frac{G_2}{G_1} = \frac{29{,}400 - 15{,}050}{29{,}400 - 8{,}750} = .70$$

For $G_1 = .783$ mph then:

$G_2 = .548$ mph

$L_1 = .548$ mph

$L_2 = .783$ mph

$$G_{Avg} = L_{Avg} = \sqrt{(.783)(.548)} = .655 \text{ mph}$$

Step 3) Predict Mass Transfer Units:

a) Gas Mass transfer units (N_G)

N_G is calculated using the AIChE University of Michigan(13) equation:

$$N_G = \frac{525 \quad D_G^{0.53}\, \rho_G^{\frac{1}{2}}\, F^{n-1}\left(H_f - H_c\right)^{0.72}}{\rho_L^{0.83}}$$

Where $n = 0.85 \left(\frac{\mu_L}{\rho_L}\right)^{0.24}$

$D_G = .515 \text{ ft}^2/\text{hr}$

$\rho_G = .184 \text{ lbs/ft}^3$

$\mu_L = .605 \text{ lbs/ft hr}$

$\rho_L = 48.6 \text{ lbs/ft}^3$

$G_{Avg} = 0.655 \text{ moles/hr}$

$P = 1 \text{ atm}$

$T = 691°F$

$A_T = 0.129 \text{ ft}^2$

$$V_S(\text{Average}) = \frac{G_{Avg}\ (379)(144)}{3600(18.6)} \times \frac{T}{520} \times \frac{1}{P} = \frac{.655(379)(691)(144)}{3600(18.6)(520)} = .710 \text{ ft/sec}$$

V_S is based on A_T since this is also area of annuluar space above the liquid on the tray.

$$F = V_S \sqrt{\rho_G} = .710 \sqrt{.184} = .304$$

$$n = .85 \left(\frac{\mu_L}{\rho_L}\right)^{.24} = .85 \left(\frac{.605}{48.6}\right)^{.24} = .35$$

$$H_c = .825 - .65\ (F) + .0226\ L_{Avg} = .825 - .65\ (.304) + .0226\ (.655)$$

$= .644$ inches (See thesis Page 32, Equation-21.)

$\frac{H_c}{H_f} = f(F) = .583$ (From Michigan report(13) Figures 4-27)

$$\therefore H_f = \frac{.644}{.583} = 1.103 \text{ inches}$$

$H_f - H_c = .459$ inches

Terms for N_G equation are:

$$D_G^{.53} = .703$$

$$\rho_G^{.50} = .429$$

$$\rho_L^{.83} = 25.0$$

$$F^{n-1} = F^{-.65} = 2.17$$

$$\left(\frac{H_f - H_c}{12}\right)^{.72} = .0952$$

$$\therefore N_G = \frac{525(.703)(.429)(2.17)(.0952)}{25} = 1.31$$

b) Liquid Mass Transfer Units

N_L is calculated using the AIChE University of Michigan(13) equation:

$$N_L = 42\ D_L^{0.48}\ F^{0.58}\ \theta_L$$

Where: $D_L = 7.29(10^{-4})\text{ft}^2/\text{hr}$

$F = .304$

$A_T = 18.6$ sq. inches

$H_c = .644$ inches

$L_{Avg} = .655$ mph

$\rho_L = 48.6$ lbs/ft

Terms for N_L equation are:

$$D_L^{.48} = .0312$$

$$F^{.58} = .50$$

$$\therefore N_L = 42(3600)\frac{(48.6)}{92.13}(.0312)(.50)\left(\frac{.644}{12}\right)\left(\frac{18.6}{144}\right) \times \frac{1}{.655} = 13.20$$

Step 4) Predict Eddy Diffusivity

D_E = 12 (See Discussion of Results Thesis Page 33)

Step 5) Determine y_2/x_2 By Running Program

Input to Program:

Symbol	Definition	Value
DE	Eddy Diffusivity	12.0
RHOL	Molal Density of Liquid on Tray	0.528
RHOF	H_c/H_f, $\frac{\text{Cubic feet of liquid}}{\text{Cubic feet of froth}}$	0.615
Z1	Z_t, Tray Flow Path Length, feet	0.620
A	A_c, Cross-Section of Liquid Flow Path	
	W_tH_f, sq. ft.	0.0192
G_1	G_1, Inlet Vapor Rate, lb moles/hr	0.783
EL_1	L_1, Inlet Liquid Rate, lb moles/hr	0.548
Delta L	Δ, Condensation Rate, lb moles/hr	0.235
W	w, Fractional Flow Path Length for x	1.0
EM	m, Equilibrium Constant	43.5
ENL	N_L, Liquid Mass Transfer Units	13.20
ENG	N_G, Gas Mass Transfer Units	1.31

Predicted y_2/x_2 = 167

APPENDIX SECTION D
COMPARISON OF NEW EQUATIONS TO CONVENTIONAL EQUATIONS AT CONSTANT MOLAL FLOW

Point Separation

The new point degree of separation Equation-13A is evaluated at constant molal flow by taking the limit of the equation as the rate of condensation ($\triangle$) approaches zero. As is shown below, the result is that $\lim\limits_{\triangle\to 0}$ (Equation-13A) = Equation-13B; 13B being the conventional constant molal Murphree point efficiency equation.

First considering the left hand side of 13A:

$$\lim_{\triangle\to 0} \frac{y'_2-y_1}{\frac{y^*}{b_1}-y_1} = \frac{y'_2-y_1}{\frac{y^*}{\lim\limits_{\triangle\to 0} b_1}-y_1} \tag{Ap-1}$$

Where:

$$\lim_{\triangle\to 0} b_1 = \lim_{\triangle\to 0}\left[m+(1-m)\, e^{\frac{\triangle}{L\cdot N_L}}\right] = 1+\cancel{m}-\cancel{m} = 1 \tag{Ap-2}$$

$$\therefore \lim_{\triangle\to 0} \frac{y'_2-y_1}{\frac{y^*}{b_1}-y_1} = \frac{y'_2-y_1}{y^*-y_1} = \text{left hand side of 13B} \tag{Ap-3}$$

Considering the right hand side of 13A:

$$\lim_{\triangle\to 0}\left[1-e^{\left(\frac{b_1}{b_2-b_1}\ell n\frac{G_{1-\triangle}}{G_1}\right)}\right] = 1-e^{\left[\lim\limits_{\triangle\to 0}\frac{b_1}{b_2-b_1}\ \ell n\ \frac{G_{1-\triangle}}{G_1}\right]} \tag{Ap-4}$$

Where:

$$\lim_{\Delta\to 0} \frac{b_1}{b_2-b_1} \ln \frac{G_{1-\Delta}}{\Delta} = \lim_{\Delta\to 0} \frac{\left[m+(1-m)\, e^{\frac{\Delta}{L.N_L}}\right] \ln \frac{G_{1-\Delta}}{G_1}}{m+(1-m)\, e^{\frac{\Delta}{L.N_L}} - e^{\frac{\Delta}{L.N_L}}\, e^{\frac{\Delta}{G.N_G}}}$$

$$= \frac{(m-m+1)(0)}{m-m+1-1} = \frac{0}{0} \qquad \text{(Ap-5)}$$

Now according to L'Hospital's rule when $\lim\limits_{x\to c} \frac{f(x)}{g(x)} = \frac{0}{0}$, which is indeterminate, the true value of this limit is given by:

$$\lim_{x\to c} \frac{f(x)}{g(x)} = \frac{\lim\limits_{x\to c} \frac{df(x)}{dx}}{\lim\limits_{x\to c} \frac{dg(x)}{dx}}$$

Applying this rule to Ap-5 :

$$\lim_{\Delta\to 0} \frac{b_1 \ln \frac{G_{1-\Delta}}{G_1}}{b_2-b_1} = \frac{\lim\limits_{\Delta\to 0} d\left(b_1 \ln \frac{G_{1-\Delta}}{G_1}\right) \Big/ \cancel{d\Delta}}{\lim\limits_{\Delta\to 0} d\left(b_2-b_1\right) \Big/ \cancel{d\Delta}} \qquad \text{(Ap-6)}$$

First evaluating the numerator of Ap-6 :

$$\lim_{\Delta\to 0} d\left(b_1 \ln \frac{G_{1-\Delta}}{G_1}\right) = \lim_{\Delta\to 0} \left[\frac{-m}{G_1-\Delta} - \frac{(1-m)}{G_1} + \frac{(1-m)\left(e^{\frac{\Delta}{L.N_L}}\right) \ln\left(G_{1-\Delta}\right)}{L.N_L} - \frac{(1-m)\left(e^{\frac{\Delta}{L.N_L}}\right) \ln G_1}{L.N_L}\right] = \frac{-m}{G_1} - \frac{1-m}{G_1} + \frac{(1-m)\ln G_1}{L.N_L} - \frac{(1-m)\ln G_1}{L.N_L} =$$

$$\frac{-1}{G_1} = \frac{-1}{G} \qquad \text{(Ap-7)}$$

For the denominator of AP-6:

$$\lim_{\Delta\to 0} d(b_2-b_1) = \lim_{\Delta\to 0}\left[\frac{e^{\frac{\Delta}{L.N_L}}\, e^{\frac{\Delta}{G.N_G}}}{L.N_L} + \frac{e^{\frac{\Delta}{L.N_L}}\, e^{\frac{\Delta}{G.N_G}}}{G.N_G} - \frac{(1-m)\, e^{\frac{\Delta}{L.N_L}}}{L.N_L}\right]$$

$$= \frac{1}{L.N_L} + \frac{1}{G.N_G} - \frac{(1-m)}{L.N_L} = \frac{1}{G.N_G} + \frac{m}{L.N_L} \qquad \text{(Ap-8)}$$

Substituting AP-7 and Ap-8 in Ap-6 gives:

$$\lim_{\Delta\to 0} \frac{b_1 \,\ln \frac{G_{1-\Delta}}{G_1}}{b_2-b_1} = \frac{-1}{\frac{1}{N_G} + \frac{mG}{L.N_L}} = \frac{-1}{\frac{1}{N_{OG}}} = -N_{OG} \qquad \text{(Ap-7)}$$

Substituting Ap-7 in Ap-4:

$$\lim_{\Delta\to 0}\left[1-e^{\left(\frac{b_1}{b_2-b_1}\ln\frac{G_{1-\Delta}}{G_1}\right)}\right] = 1-e^{-N_{OG}} = \text{right hand side of 13B} \qquad \text{(Ap-8)}$$

Ap-8 in conjunction with Ap-3 prove that $\lim_{\Delta\to 0}$ (Eqn-13A) = Equation-13B.

Plate Separation

The new plate degree of separation Equation-18 is shown below to be numerically in agreement (±0.3%) to the AIChE(7) eddy diffusion equation. An analytical comparison is not practical since Equation-18 was integrated by a series technique while the AIChE was not. The AIChE equation is given below:

$$\frac{y_2-y_1}{y^*-y_1} = E_{OG}\left[\frac{1-e^{\left(-n-N_{Pe}\right)}}{\left(n+N_{Pe}\right)\left(\frac{1+n+N_{Pe}}{n}\right)} + \frac{e^{n}-1}{n\left(1+\frac{n}{n+N_{Pe}}\right)}\right] \qquad \text{(Ap-9)}$$

Where:

$$n = \frac{N_{Pe}}{2}\left[\sqrt{1+\frac{4mG_1E_{OG}}{L_1\left(N_{Pe}\right)}}\ -1\right]$$

and $$N_{Pe} = \frac{Z_tL_1}{D_EA_c\rho_{LM}H_c \big/ H_f}$$

At constant molal flow the "C" terms in Equation-18 reduce to $C_1 = (N_{Pe})\left(\frac{mG_1}{L_1}\right)(E_{OG})$; $C_2 = N_{Pe}$, $C_3 = 0$, $C_4 = N_{Pe}\frac{G_1}{L_1}E_{OG}$. Thus, in both cases the degree of separation is a function only of the terms: N_{Pe}, m, $\frac{G_1}{L_1}$, and E_{OG}. For the purpose of comparison, the following constant molal flow examples have been worked using the AIChE Equation Ap-9 by hand calculation and Equation-18 via FORTRAN program in Appendix B.

Case	N_{Pe}	m	G_1/L_1	E_{OG}	AIChE	Eqn. 18
1	.10	10	1.0	.10	1.900	1.900
2	1.0	10	1.0	.10	2.030	2.025
3	10.0	10	1.0	.10	2.359	2.366
4	6.8	43.5	1.0	.197	169.2	168.9

All these cases are at total reflux, i.e., $\frac{G_1}{L_1} = 1.0$, and thus y_2/x_2 can be calculated independent of composition. As can be seen, the agreement of y_2/x_2 predictions in the arbitrarily selected Cases 1-3, is quite good, i.e., $<0.3\%$ deviations. Case 4, a spot-check of the constant molal flow case of this thesis experiment, shows less than a 0.20% deviation. These minor deviations appear to be due mostly to the inaccuracy of hand calculating the AIChE equation.

The lower the Peclet number (N_{Pe}), the greater the degree of mixing on a plate. In Case 1, the N_{Pe} value is sufficiently low such that the y_2/x_2 value predicted by Equation-18, and the AIChE equation, is what is obtained by just using the E_{OG} Equation-13B directly. Thus Equation-18, like the AIChE model, appears to reduce to the E_{OG} equation at total mixing.

APPENDIX SECTION E
ROTAMETER CALIBRATION

Reflux flows were measured by means of a rotameter. At 100% flow the rotameter was rated to be able to pass 0.81 GPM of a 1.0 specific gravity liquid. Since toluene was used at various temperatures (specific gravities not equal to 1.0) it was necessary to calibrate the rotameter.

Referring to Brown(16), the following equation was used as the basis for calibration:

$$W = C_R A_o \sqrt{\frac{2g\rho\ (\rho_f - \rho)\ V_f}{A_f}} \qquad \text{(Ap-10)}$$

Where: W = Weight flow/unit time

C_R = Coefficient of discharge

A_o = Area of the annular opening between the largest cross-section of the float and the wall of the tube at any point.

g = Gravitational constant

ρ = Fluid density

ρ_f = Density of the float

V_f = Volume of the float

A_f = Maximum cross-sectional area of the float

Setting up two relationships, one for water and one for toluene, assuming C_R is essentially constant, and equating, yields the following expression:

$$\frac{W_1^2}{W_2^2} = \frac{\rho_1\ (\rho_f - \rho_1)}{\rho_2\ (\rho_f - \rho_2)} \qquad \text{(Ap-11)}$$

Where: W_1 = 6.75#/minute (Water)

ρ_1 = 1.00 (Sp.G of Water)

ρ_f = 8.02 (Sp.G of Stainless Steel Float)

W_2 = Toluene Weight Flow, #/Minute

ρ_2 = Toluene Sp.G

Substituting fixed values in Ap-11 yields:

$$W_2 = 2.55\sqrt{\rho_2\ (8.02-\rho_2)} \qquad \text{(Ap-12)}$$

Solving for 100% toluene flow at various temperatures:

T, °F	ρ_2	W_2, #/Min
80	0.862	6.35
100	0.852	6.30
150	0.825	6.22
180	0.809	6.16
200	0.798	6.12
231	0.780	6.06

APPENDIX SECTION F

REFERENCES

(1) Murphree, E. V., Ind. Eng. Chem., 1925, V117, pg 747.

(2) Nord, M., Trans. Am. Inst. Chem. Engrs., 1946, V42, pg 863.

(3) Treybal, R. E., Mass Transfer Operations, McGraw Hill, 1955, pg 228.

(4) Kent, E. R. and Pigford, R. L., AIChE Journal, 1956, V3, N2, pg 303.

(5) Colburn, A. P. and Drew, T. B., Trans. Am. Inst. Chem. Engrs., 1937, V33, pg 197.

(6) Anderson, J. E., Sc.D. Thesis, Mass. Inst. Tech., Cambridge, 1954.

(7) AIChE Research Committee Final Report on Tray Efficiency, University of Delaware, 1958.

(8) Rukenshtein, E. S., J. Applied Chem. (USSR), 1957, V30, pg 1012.

(9) Whitman, W. G., Chem. Met. Eng., 1923, V29, pg 146.

(10) Mitchell, J., Jr. and Smith, D. M., Aquametry, Interscience Publishers, Inc., New York, 1948.

(11) Slattery, J. C. and Bird, R. B., AIChE Journal, 1958, V5, N4, pg 137.

(12) Wilke, C. R. and Chang, P., AIChE Journal, 1955, V2, N1, pg 264.

(13) AIChE Research Committee - Tray Efficiencies in Distillation Columns, Univ. of Michigan Final Report, 1960.

(14) Gilbert, T. J., Chem. Eng. Science, 1959, V10, pg 243.

(15) Barker, P. E., and Self, M. F., Chem. Eng. Science, 1962, V17, pg 541.

(16) Brown, G. G., et al, Unit Operations, John Wiley & Sons, 1950, pg 161.

(17) Pickles, D. E., M. S. Thesis, Mass. Inst. Tech., Cambridge, 1954.

(18) Gester, G. C., CEP, 1947, V43, No. 3, pg 117.

(19) Hibbard and Schalla, Solubility of Water in Hydrocarbons, Natl. Advisory Comm. Aeronautics, NACA Res. Memo RME52 D24, July 10, 1952.

(20) Maxwell, J. B., Data Book on Hydrocarbons, D. Van Nostrand Co., Inc., New York, 1950.

(21) Holland, C. D., Multicomponent Distillation, Prentice-Hall, 1963.